

NAVSWC TR 91-326

AD-A252 397



**PSEUDOPOTENTIAL BAND CALCULATIONS  
ALONG A HIGH-SYMMETRY AXIS: PART II  
Spin-Orbit Interaction and the [111] Direction**

BY D. Y. AGASSI and J. B. RESTORFF

RESEARCH AND TECHNOLOGY DEPARTMENT

1 JULY 1991



Approved for public release; distribution is unlimited.



**NAVAL SURFACE WARFARE CENTER**

Dahlgren, Virginia 22448-5000 • Silver Spring, Maryland 20903-5000

**92-17131**



92

6

1-13

**PSEUDOPOTENTIAL BAND CALCULATIONS  
ALONG A HIGH-SYMMETRY AXIS: PART II  
Spin-Orbit Interaction and the [111] Direction**

**BY D. Y. AGASSI and J. B. RESTORFF  
RESEARCH AND TECHNOLOGY DEPARTMENT**

**1 JULY 1991**

Approved for public release; distribution is unlimited.

**NAVAL SURFACE WARFARE CENTER**

**Dahlgren, Virginia 22448-5000 • Silver Spring, Maryland 20903-5000**

**FOREWORD**

A cylindrical coordinates approach to phenomenological band structure calculations introduced previously is generalized to include spin degrees of freedom and the spin orbit interaction. The pertaining reduction of the Schrodinger equation to a set of 1-d wave equations is derived. For the test case of PbSe band along the  $\Gamma$ -L line, the correct bands are reproduced in the numerically-stable range of parameters.

The authors would like to acknowledge Dr. J. R. Cullen for useful discussions. This work was supported by the Office of Naval Research and the Naval Surface Warfare Center's Independent Research Fund.

Approved by:

*Carl W. Larson*

CARL W. LARSON, Head  
Physics and Technology Division

<b>Accession For</b>	
NTIS GRA&I	<input checked="" type="checkbox"/>
DTIC TAB	<input type="checkbox"/>
Unannounced	<input type="checkbox"/>
Justification	
By	
Distribution/	
<b>Availability Codes</b>	
<b>Dist</b>	<b>Avail and/or Special</b>
A-1	

ABSTRACT

A rapidly convergent method for band structure calculations, based on a cylindrical coordinates expansion, is generalized to include the spin-orbit interaction. This approach is advantageous particularly for materials highly anisotropic in one direction. The pertinent wave equations are tested for the PbSe low bands along the  $\Gamma$ -L line. The results compare well with PbSe known band structure except where the bands group together to form degenerate, or near degenerate, equal parity clusters.

# CONTENTS

<u>Section</u>	<u>Page</u>
1 INTRODUCTION . . . . .	1-1
2 CYLINDRICAL COORDINATES MULTIPOLE EXPANSIONS IN THE PRESENCE OF SPIN . . . . .	2-1
3 SYMMETRY PROPERTIES . . . . .	3-1
4 THE MULTIPOLES WAVE EQUATIONS . . . . .	4-1
5 BAND STRUCTURE OF PbSe IN THE $\Gamma$ -L ([111]) DIRECTION . .	5-1
THE SPIN-ORBIT INTERACTION . . . . .	5-1
RESULTS FOR PbSe ALONG THE [111] DIRECTION . . . . .	5-5
6 SUMMARY AND DISCUSSION . . . . .	6-1
REFERENCES . . . . .	7-1
DISTRIBUTION . . . . .	(1)

<u>Appendix</u>	<u>Page</u>
A IRREDUCIBLE REPRESENTATIONS OF THE DOUBLE GROUPS $C_{3v}^{(d)}$ AND $D_{3d}^{(d)}$ . . . . .	A-1
B MULTIPOLE CONTENT OF THE $C_{3v}^{(d)}$ AND $D_{3d}^{(d)}$ SPIN REPRESENTATIONS . . . . .	B-1
C DERIVATION OF EQUATION (4-3) . . . . .	C-1
D MODELS FOR THE SPIN-ORBIT VECTOR FORM FACTOR . . . . .	D-1
E NUMERICAL SOLUTION OF THE MULTIPOLE WAVE EQUATION . . .	E-1

# ILLUSTRATIONS

<u>Figure</u>		<u>Page</u>
5-1	CALCULATED BAND STRUCTURES OF PbSe ALONG THE Γ-L DIRECTION . . . . .	5-6
5-2	THE DEPENDENCE OF NEAR-E <sub>F</sub> BANDS AT THE L-POINT ON THE SPIN-ORBIT STRENGTH S <sub>ND</sub> = SD < 0 . . . . .	5-8

# TABLES

<u>Table</u>		<u>Page</u>
1-1	STRUCTURE OF fcc g-HEXAGONS ASSOCIATED WITH THE [111] DIRECTION . . . . .	1-2
3-1	MULTIPOLE CONTENT OF THE IRREDUCIBLE SPIN REPRESENTATIONS OF C <sub>3v</sub> . . . . .	3-2
3-2	MULTIPOLE CONTENT OF THE IRREDUCIBLE SPIN REPRESENTATIONS OF D <sub>3d</sub> <sup>(d)</sup> . . . . .	3-3
5-1	SYMMETRY PROPERTIES OF THE SPIN-ORBIT FROM FACTOR $\vec{f}_m(g_p, z')$ . . . . .	5-2
5-2	BLOCK STRUCTURE OF WAVE EQUATIONS (4-3) . . . . .	5-3
5-3	SPIN-ORBIT PARAMETERS . . . . .	5-4
5-4	BAND ENERGY DEPENDENCE ON SPIN-ORBIT PARAMETERS AT THE L-POINT L <sub>6</sub> <sup>±</sup> . . . . .	5-7
A-1	IRREDUCIBLE SPIN REPRESENTATIONS OF C <sub>3v</sub> <sup>(d)</sup> . . . . .	A-4
A-2	IRREDUCIBLE SPIN REPRESENTATIONS OF D <sub>3d</sub> <sup>(d)</sup> . . . . .	A-5

## SECTION 1

## INTRODUCTION

In a previous paper<sup>1</sup> (hereafter referred to as I), we introduced a method for band structure calculations along a high-symmetry axis. The method constitutes of expanding the wave function (and potential) in cylindrical coordinate multipole and reducing the three-dimensional Schrodinger equation to a set of coupled one-dimensional wave equations for these multipoles. The primary advantage of the method is its good convergence, in particular for anisotropic systems with a unit cell largely extending in one direction,  $\hat{z}'$ . Examples for such systems are superlattices, intercalates, and a lattice bounded by a surface. The method applies equally to bulk band calculations along a high-symmetry axis. In this paper we generalize the method to include spin degrees of freedom. Such an extension is necessary in situations where the spin-orbit (SO) interaction is important. A case in point, the heavy-element narrow gap semiconductors belonging to the II-VI and IV-VI systems.<sup>2</sup> For these materials, the SO interaction is essential to correctly obtain the band gap.<sup>3</sup> Another application is the calculation of g-factors where the inclusion of spin degrees of freedom is obviously indispensable. We outline first the method without spin and point out the modifications mandated by the presence of the spin degrees of freedom. We then comment on the main points borne out by the band calculation of PbSe, which serves as a test case.

At the core of the method is the cylindrical multipole expansion of lattice periodic functions.<sup>1</sup> Examples of such functions are band wave functions, the pseudopotential, and the spin-orbit form factor. These multipoles follow naturally from the introduction of cylindrical coordinates, chosen such that its z-axis coincides with  $\hat{z}'$ , the high-symmetry axis. For example, the multipole expansion of a band wave function  $\Psi(\vec{r}')$  where the crystal's momentum  $\vec{k}$  points at the  $\hat{z}'$ -direction is<sup>1</sup>

$$\Psi(\vec{r}') = \sum_{g_F} \sum_{\ell=-\infty}^{\infty} \Psi_{\ell}(g_F, z') J_{\ell}(g_F \rho) e^{i\ell\phi} \quad (1-1)$$

In Equation (1-1),  $g_F$  runs over a series of lattice-specific nonnegative values (Table 1-1),  $J_{\ell}(x)$  is the Bessel function of order  $\ell$  and  $(\rho, \phi, z')$  are the standard cylindrical coordinates. Rapid convergence of Equation (1-1) implies that a small number of distinct multipoles  $\Psi_{\ell}(g_F, z')$  yields a good description of  $\Psi(\vec{r}')$ .

TABLE 1-1. STRUCTURE OF fcc g-HEXAGONS ASSOCIATED WITH THE [111] DIRECTION

$$g = f/a \quad (\text{in } \text{\AA}^{-1})$$

	f	$g(\text{PbSe})^{(a)}$	$\Phi_0(g)$ (degrees)
1.	0.	0.	0.
2.	$10.2606 = 2\pi\sqrt{\frac{8}{3}}$	1.6754	0.
3.	$17.7714 = 2\pi\sqrt{8}$	2.9018	30
4.	$20.5207 = 2\pi\sqrt{\frac{32}{3}}$	3.3507	0.
5.	27.1465	4.4326	19.1066
6.	30.7813	5.0261	0.
7.	35.5430	5.8036	30
8.	36.9944	6.0406	13.8979
9.	41.0414	6.7014	0.
10.	44.7239	7.3027	36.5868
11.	47.0193	7.6775	10.8934

(a) We used<sup>1</sup>  $a(\text{PbSe}, T = 300\text{K}) = 6.1243 \text{ \AA}$

NOTE: The  $g$  values and  $\Phi_0(g)$  angle (Equation (3-1)) for the PbSe (fcc) lattice in the [111] direction.<sup>1</sup>



The convergence of Equation (1-1) hinges on two general properties, which severely limits the number of contributing  $\ell$  and  $g_F$  indices. The  $\ell$  variation is controlled by the symmetry of the  $z'$ -axis. For example, group-theoretic considerations imply that for a fcc lattice and  $\hat{z}' \parallel [111]$  only two  $\ell$  values need be considered.<sup>1</sup> All other multipoles are phase related to those two multipoles. As a consequence, expansion (1-1) is in effect an expansion in  $g_F$ . The  $g_F$  expansion, in turn, is controlled by an energy-geometry argument. To see this point, note that in Equation (1-1) the transversal behavior of  $\Psi(\vec{r}')$  is controlled by the oscillations of  $J_\ell(g_F \rho)$ , with period  $g_F^{-1}$ .<sup>4</sup> Therefore for "low" band energies, the important terms in Equation (1-1) involve only the lowest  $g_F$ -values, up to a cutoff value  $g_C$ . Based on the behavior of the  $J_\ell(x)$  curve, the latter has been estimated in I to satisfy  $(\ell + 3/2)/g_C \approx .5 a_T$  where  $\ell$  is a typical  $\ell$ -value and  $a_T$  is of the order of the lattice constant in the transversal direction. For the PbSe example (see I),  $g_C$  turns to be approximately the second  $g$  value (see Table 1-1; the first  $g$  value,  $g = 0$ , always contributes). Thus both the  $\ell$  and  $g$  variation in expansion Equation (1-1) are severely restricted, hence the rapid convergence. It is important to emphasize that the above considerations are valid regardless of the extension of the unit cell in the  $\hat{z}'$  direction! In particular, the good convergence of Equation (1-1) applies equally for bulk materials and superlattices provided they share the same high symmetry axis  $\hat{z}'$ . The validity of these arguments has been numerically tested in I for a simple case.

The second important ingredient of the method is the simplicity of the pertinent wave equations for  $\Psi_\ell(g, z')$ .<sup>1</sup> This is a set of coupled, one-dimensional second-order ordinary differential equations (in  $z'$ ). The coupling potentials are derivable from the underlying three-dimensional pseudopotential by means of geometrical coefficients, the "A-coefficients" (see I). These equations are reminiscent of a set of coupled Kronig-Penney models.<sup>5</sup> They can be solved by any convenient algorithm such as straight integration (when the energy is not too low), or via conversion into a secular matrix.

With spin degrees of freedom the features just discussed hold, though some of the details change. An obvious modification is that with spin, the wave function is comprised of two components pertaining to the two possible spin projections. Consequently, two multipole expansions such as Equation (1-1) need be considered simultaneously, and the total number of relevant multipoles roughly doubles. The corresponding wave function for the multipoles include additional terms (in comparison to the no-spin counterpart), one of which is a first order derivative (Section 4). The SO effect is primarily mixing the two spin components of the wave function. In the present phenomenological approach, this mixing is controlled by adjustable parameters. The relative ease of including SO is an attractive feature of the present method.

To demonstrate how the method works, and as a first application, we consider the PbSe band structure along the [111] direction. The analysis demonstrates several points:

1. Group-theoretic considerations directly indicate the SO-induced admixtures. In particular, we recover the effect of band gap reduction by the SO interaction.

2. We correctly obtain the low bands throughout most of the  $\Gamma$ -L line. Numerical artifacts, however, limit at present the method to non-degenerate bands.

3. The spin-orbit interaction depends on two phenomenological parameters, roughly corresponding to the ( $\ell=0$ ,  $j=1/2$ ) and ( $\ell=1$ ,  $j=1/2, 3/2$ ) SO strengths.

The paper is organized as follows. In Section 2 we introduce the multipole expansion in the presence of spin. In Section 3 we discuss the group-theoretic considerations pertaining to the cylindrical multipoles. Section 4 is devoted to the derivation of the central wave equations for the multipoles. The last section describes the results of numerical calculation for PbSe bands in the  $\Gamma$ -L direction and a brief discussion. Most of the technical details are given in the appendices.

## SECTION 2

## CYLINDRICAL COORDINATES MULTIPOLE EXPANSIONS IN THE PRESENCE OF SPIN

The formalism described in I is extended here to include spin. In the unprimed coordinates (x,y,z), the spin wave function is a spinor ( $\chi(\sigma)$ ) where ( $\chi(1)$ ) and ( $\chi(-1)$ ) designate the "spin-up" and "spin-down" states, respectively. Hereafter, we adopt the notation that parentheses around a function or operator indicate a spinor, such as for ( $\chi(\sigma)$ ). Using this notation, a spinor Bloch function in the unprimed coordinates ( $\Psi_{\vec{n}\vec{k}}(\vec{r})$ ) has the form<sup>6</sup>

$$(\Psi_{\vec{n}\vec{k}}(\vec{r})) = e^{i\vec{k}\cdot\vec{r}} (U_{\vec{n}\vec{k}}(\vec{r})) \quad (2-1)$$

where the lattice-periodic spinor ( $U_{\vec{n}\vec{k}}(\vec{r})$ ) has the decomposition<sup>7</sup>

$$(U_{\vec{n}\vec{k}}(\vec{r})) = \sum_{\sigma=\pm 1} U_{\vec{n}\vec{k}}^{(\sigma)}(\vec{r}) (\chi(\sigma)) = \begin{bmatrix} U_{\vec{n}\vec{k}}^{(+)}(\vec{r}) \\ U_{\vec{n}\vec{k}}^{(-)}(\vec{r}) \end{bmatrix} \quad (2-2)$$

To derive the multipole expansion of Equation (2-1) we first transform to the primed coordinates where  $\hat{z}'$  points at the direction of a high-symmetry axis. Such a rotation affects also the spinors since

$$\hat{R} [\Psi(\vec{r})(\chi)] = [\hat{R} \Psi(\vec{r})] [\hat{R}(\chi)] \quad (2-3)$$

where  $\hat{R}$  is the rotation operator, and  $\Psi(\vec{r})$  and  $\chi$  are an arbitrary function and spinor, respectively. The spinor factor  $[\hat{R}(\chi)]$  transforms according to the  $D^{1/2}(\alpha, \beta, \gamma)$  two-dimensional matrix<sup>6,8</sup> where  $\alpha, \beta, \gamma$  are the Euler angles. The radial factor  $[\hat{R}\Psi(\vec{r})] = \Psi(\vec{R}^{-1}\vec{r}')$  has been discussed in I. As in I, we limit ourselves to crystal momentum  $\vec{k}'$  such that  $\vec{k}'\cdot\vec{r}' = k'z'$ . Therefore, in the primed coordinates

$$(\Psi_{\vec{n}\vec{k}'}(\vec{r}')) = e^{ik'z'} \sum_{\sigma} U_{\vec{n}\vec{k}'}^{(\sigma)}(\vec{r}') (\chi'(\sigma)) \quad (2-4)$$

where  $U_{\vec{n}\vec{k}'}^{(\sigma)}(\vec{r}')$  are linear combinations of  $U_{\vec{n}\vec{k}}^{(\sigma)}(\vec{r})$  and the spinors ( $\chi'(\sigma)$ ) refer to the  $\hat{z}'$ -direction. For the [111] direction in particular

$$0 < k' = K \frac{3\pi}{a^*}$$

$$0 < K \leq 1, \quad a^* = a\sqrt{3} \quad (2-5)$$

The form Equation (2-4) involves two lattice-periodic functions. Therefore in analogy to Equation (1-1) (see I), they have the following multipole expansion

$$(\Psi_{\vec{n}\vec{k}',(\vec{r}')}^{(\sigma)}) = \sum_{\sigma=\pm 1} \sum_{g_F} \sum_{\ell=-\infty}^{\infty} \Psi_{\ell}^{(\sigma)}(g_F, z') J_{\ell}(g_F \rho) e^{i\ell\phi} (\chi'(\sigma)) \quad (2-6)$$

where the two spin multipoles are given by

$$\begin{aligned} \Psi_{\ell}^{(\sigma)}(g_F, z') &= i^{\ell} \sum_{\vec{L}'} \Psi^{(\sigma)}(\vec{L}') e^{i(k'+L'_z) z'} e^{-i\ell \delta(L'_T)} \\ |\vec{L}'_T| &= g_F \end{aligned} \quad (2-7)$$

In Equation (2-7)  $\vec{L}'$  denoted a reciprocal lattice vector in the primed coordinates,  $\vec{L}'_T$  is its transversal (normal to  $z'$ ) component,  $\Psi(\vec{L}')$  are the Fourier coefficients of  $\Psi(\vec{r}')$ , and the shift phase  $\delta(\vec{L}'_T)$  is defined in I.

We turn now to the SO interaction. The goal is to cast it in a form compatible with expansions of the structure Equations (2-6) and (2-7).

In the unprimed coordinates and cgs units, the spin orbit interaction is given by<sup>6,9</sup>

$$(\hat{V}_{SO}(\vec{r})) = \frac{-i \hbar^2}{4m_0 c^2} \left[ \hat{\vec{\sigma}} \cdot (\vec{\nabla} V(\vec{r}) \times \vec{\nabla}) \right] \quad (2-8)$$

In Equation (2-8) the Pauli-matrices "vector" is  $\hat{\vec{\sigma}} = (\hat{\sigma}_x, \hat{\sigma}_y, \hat{\sigma}_z)$  and  $V(\vec{r})$  is the proper ionic lattice-periodic potential. The details of  $V(\vec{r})$  are unknown. However, in the ionic core portion of space, where its derivative is the largest, it is customarily approximated by a Coulombic potential  $V_c(r)$  with a form factor. For an ion at  $\vec{r} = 0$ , it follows that  $\vec{\nabla} V(\vec{r}) \approx \vec{\nabla} V_c(\vec{r}) = \frac{|e|^2 Z}{r^3} \vec{r}$

where  $Z$  is the effective ionic charge. Consequently, Equation (2-8) takes the standard form

$$(\hat{V}_{SO}(\vec{r}))_{|\vec{r}| \rightarrow 0} = \frac{\hbar^2}{4m_0 c^2} \frac{|e|^2 Z}{r^3} (\hat{\vec{\sigma}} \cdot \hat{\vec{r}}) \quad (2-9)$$

where the angular momentum is  $\hat{\vec{L}} = -i\vec{r} \times \vec{\nabla}$ .

For a lattice-periodic array of ions, a natural generalization of Equation (2-9) is

$$(\hat{V}_{SO}(\vec{r})) = \sum_i f_i(|\vec{r} - \vec{r}_i|) (\hat{\vec{\sigma}} \cdot \hat{\vec{L}} (\vec{r} - \vec{r}_i)) \quad (2-10)$$

where  $\vec{r}_i$  runs over all atomic positions in the crystal and  $f_i(|\vec{r} - \vec{r}_i|)$  is a phenomenological form factor. This form is readily transformed to the primed coordinates since  $(\hat{\vec{\sigma}} \cdot \hat{\vec{L}}) = (\hat{\vec{\sigma}}' \cdot \hat{\vec{L}}')$  and distances  $|\vec{r} - \vec{r}_i|$  are conserved by rotations. In addition, since the nonderivative factors in Equation (2-10) are lattice-periodic, the Fourier expansion of the SO form factor in the primed coordinates is

$$\vec{f}(\vec{r}') = \sum_i f_i(|\vec{r}' - \vec{r}_i'|) (\vec{r}' - \vec{r}_i') = \sum_{\vec{G}'} \vec{f}(\vec{G}') e^{i\vec{G}' \cdot \vec{r}'} \quad (2-11)$$

and the SO interaction Equation (2-10) takes the convenient form

$$(\hat{V}_{SO}(\vec{r}')) = -i (\hat{\vec{\sigma}}' \cdot [\sum_{\vec{G}'} \vec{f}(\vec{G}') e^{i\vec{G}' \cdot \vec{r}'} \times \vec{\nabla}']) \quad (2-12)$$

The form Equation (2-12) is mathematically convenient. Its operation on products of the type  $e^{i\vec{G}' \cdot \vec{r}'} (\chi'(\sigma))$ , as in Equation (2-7), is easily evaluated. It also naturally introduces the multipoles of the SO vector form factor Equation (2-11), i.e.,

$$\vec{f}(\vec{r}') = \sum_{g_Q} \sum_{\ell=-\infty}^{\infty} \vec{f}_{\ell}(g_Q, z') J_{\ell}(g_Q \rho) e^{i\ell\phi} \quad (2-13)$$

where in analogy to Equation (2-7) (see I, Section 2)

$$\vec{f}_{\ell}(g_Q, z') = i^{\ell} \sum_{\vec{G}'} \vec{f}(\vec{G}') e^{i\vec{G}'_z z'} e^{-i\ell\delta(\vec{G}'_T)} \quad (2-14)$$

$$|\vec{G}'_T| = g_Q$$

The  $\vec{f}_{\ell}(g_Q, z')$ , of dimensionality  $[E^{\frac{1}{2}}]$ , are the SO counterparts of the "central" pseudopotential multipoles  $v_{\ell}(g_P, z')$ .<sup>1</sup>

### SECTION 3

#### SYMMETRY PROPERTIES

The assumption that  $\hat{z}'$  is a high symmetry axis imposes severe restrictions on the allowed  $l$  values in a multipole expansion such as Equation (2-6) in part I. Lattice-periodicity in the transversal direction (normal to  $\hat{z}'$ ) yields additional constraints on the allowed  $l$  values. In this Section we consider these constraints in the presence of spin degrees of freedom. For the sake of self containment we first briefly review results from part I. Technical details are given in Appendices A and B.

Consider the multipoles of a lattice-periodic function  $W(\vec{r}')$  with Fourier components  $W(\vec{G}')$ . The origin of symmetry properties is that for a reciprocal vector  $\vec{G}' = (G_x, G_y, G_z)$  in the primed coordinates, all  $\vec{G}_T = (G_x, G_y)$  such that  $|\vec{G}_T| = g$ , lie on spokes of one or two conjugated hexagons (Figure 3-1, I). Furthermore, there are simple phase relations between  $W(\vec{G}')$  and  $W((\vec{G}')_R)$  where  $(\vec{G}')_R = ((\vec{G}'_T)_R, G_z')$ ,  $(\vec{G}'_T)_R = (G_x', -G_y')$ . These properties and the structure of a multipole Equation (2-7) lead to a situation in which, for a particular  $l$  value, either all terms in the summation Equation (2-7) cancel out or add up. As a specific example, the pseudopotential  $v(\vec{r})$ , by its very construction, is invariant under all symmetry operations of the fcc lattice. In particular, it transforms as the scalar under the  $O_h$  group and under all subgroups of  $O_h$ , such as the  $C_{3v}$  and  $D_{3d}$  groups associated with the  $[111]$  direction.<sup>10</sup> This, in turn, restricts the  $l$ -values in Equation (1-1) to  $l = 3m$ ,  $m = 0, \pm 1, \dots$  (I, Table 3-3). In addition, by virtue of the structure of the multipole  $v_l(g_p, z')$ , it is  $l$ -periodic (see I):

$$v_{l \pm 6}(g_p, z') = -e^{\pm 6i\Phi_0(g)} v_l(g_p, z')$$

$$\text{for } \sin [6\Phi_0(g)] = 0 \quad (3-1)$$

where  $\Phi_0(g)$  is given in Table 1-1. These two constraints imply that  $l = 0, 3$  are the only independent multipoles for  $v(\vec{r})$ ; all others are phase related.

In the presence of spin, the underlying symmetry groups are the double groups  $C_{3v}^{(d)}$  and  $D_{3d}^{(d)}$ <sup>6,9</sup> (see Appendix A). The corresponding  $l$  sequences are derived in Appendix B and summarized in Tables 3-1, 3-2. Note that the allowed  $l$  values for the "up" and "down" spin components are different, albeit they still belong to sequences with an

TABLE 3-1. MULTIPOLE CONTENT OF THE IRREDUCIBLE SPIN REPRESENTATIONS OF  $C_{3v}$ 

IRREDUCIBLE REPRESENTATION	$\ell$ -values <sup>(a)</sup>	$\ell$ -parity	
		$\hat{\pi}_\ell$ <sup>(b)</sup>	d
$\Lambda_4$	$ 1\rangle = \begin{bmatrix} 3m & -1 \\ 3m & +1 \end{bmatrix}$	$(-1)^{3m} \begin{bmatrix} 0 & i \\ -i & 0 \end{bmatrix}$	1
$\Lambda_5$	$ 1\rangle = \begin{bmatrix} 3m & -1 \\ 3m & +1 \end{bmatrix}$	$-(-1)^{3m} \begin{bmatrix} 0 & i \\ -i & 0 \end{bmatrix}$	1
$\Lambda_6$	$ 1\rangle = \begin{bmatrix} 3m \\ 3m & +1 \end{bmatrix},  2\rangle = \begin{bmatrix} 3m & -1 \\ 3m \end{bmatrix}$	$(-1)^{3m} \begin{bmatrix} 0 & 0 & 0 & 1 \\ 0 & 0 & 1 & 0 \\ 0 & 1 & 0 & 0 \\ 1 & 0 & 0 & 0 \end{bmatrix}$	2

(a)  $m = 0, \pm 1, \pm 2, \pm 3, \dots$

$$(b) \begin{bmatrix} U_{-\ell}(g, z') \\ V_{-\ell}(g, z') \end{bmatrix} \equiv \hat{\pi}_\ell \begin{bmatrix} U_\ell(g, z') \\ V_\ell(g, z') \end{bmatrix} \quad \text{or} \quad \begin{bmatrix} U_{-\ell}(g, z') \\ V_{-\ell}(g, z') \\ W_{-\ell}(g, z') \\ X_{-\ell}(g, z') \end{bmatrix} \equiv \hat{\pi}_\ell \begin{bmatrix} U_\ell(g, z') \\ V_\ell(g, z') \\ W_\ell(g, z') \\ X_\ell(g, z') \end{bmatrix}$$

NOTE: The  $\ell$ -sequences pertaining to the representations of the double group  $C_{3v}^{(d)}$ . The notation is explained in Appendix B.

TABLE 3-2. MULTIPOLE CONTENT OF THE IRREDUCIBLE SPIN REPRESENTATIONS OF  $D_{3d}^{(d)}$ 

IRREDUCIBLE REPRESENTATION	$\ell$ -values <sup>(a)</sup>	$\ell$ -parity $\hat{\pi}_\ell$ <sup>(b)</sup>	$z$ -parity $\hat{\pi}_z$ <sup>(c)</sup>	$d$
$L_4^+$	$ 1\rangle = \begin{bmatrix} 3m & -1 \\ 3m & +1 \end{bmatrix}$	$(-1)^{3m} \begin{bmatrix} 0 & -i \\ i & 0 \end{bmatrix}$	$(-1)^\ell \begin{bmatrix} 1 & 0 \\ 0 & 1 \end{bmatrix}$	1
$L_5^+$	$ 1\rangle = \begin{bmatrix} 3m & -1 \\ 3m & +1 \end{bmatrix}$	$-(-1)^{3m} \begin{bmatrix} 0 & -i \\ i & 0 \end{bmatrix}$	$(-1)^\ell \begin{bmatrix} 1 & 0 \\ 0 & 1 \end{bmatrix}$	1
$L_4^-$	$ 1\rangle = \begin{bmatrix} 3m & -1 \\ 3m & +1 \end{bmatrix}$	$(-1)^{3m} \begin{bmatrix} 0 & -i \\ i & 0 \end{bmatrix}$	$-(-1)^\ell \begin{bmatrix} 1 & 0 \\ 0 & 1 \end{bmatrix}$	1
$L_5^-$	$ 1\rangle = \begin{bmatrix} 3m & -1 \\ 3m & +1 \end{bmatrix}$	$-(-1)^{3m} \begin{bmatrix} 0 & -i \\ i & 0 \end{bmatrix}$	$-(-1)^\ell \begin{bmatrix} 1 & 0 \\ 0 & 1 \end{bmatrix}$	1
$L_6^+$	$ 1\rangle = \begin{bmatrix} 3m \\ 3m & +1 \end{bmatrix},  2\rangle = \begin{bmatrix} 3m & -1 \\ 3m \end{bmatrix}$	$(-1)^{3m} \begin{bmatrix} 0 & 0 & 0 & 1 \\ 0 & 0 & 1 & 0 \\ 0 & 1 & 0 & 0 \\ 1 & 0 & 0 & 0 \end{bmatrix}$	$(-1)^{3m} \begin{bmatrix} 1 & 0 & 0 & 0 \\ 0 & -1 & 0 & 0 \\ 0 & 0 & -1 & 0 \\ 0 & 0 & 0 & 1 \end{bmatrix}$	2
$L_6^-$	$ 1\rangle = \begin{bmatrix} 3m \\ 3m & +1 \end{bmatrix},  2\rangle = \begin{bmatrix} 3m & -1 \\ 3m \end{bmatrix}$	$(-1)^{3m} \begin{bmatrix} 0 & 0 & 0 & 1 \\ 0 & 0 & 1 & 0 \\ 0 & 1 & 0 & 0 \\ 1 & 0 & 0 & 0 \end{bmatrix}$	$-(-1)^{3m} \begin{bmatrix} 1 & 0 & 0 & 0 \\ 0 & -1 & 0 & 0 \\ 0 & 0 & -1 & 0 \\ 0 & 0 & 0 & 1 \end{bmatrix}$	2

(a)  $m = 0, \pm 3, \pm 6, \dots$

(b) See Table 3-3 for the definition of  $\hat{\pi}_\ell$ .

$$(c) \begin{bmatrix} U_\ell(g, -z') \\ V_\ell(g, -z') \end{bmatrix} \equiv \hat{\pi}_z \begin{bmatrix} U_\ell(g, z') \\ V_\ell(g, z') \end{bmatrix} \quad \text{or} \quad \begin{bmatrix} U_\ell(g, -z') \\ V_\ell(g, -z') \\ W_\ell(g, -z') \\ X_\ell(g, -z') \end{bmatrix} \equiv \hat{\pi}_z \begin{bmatrix} U_\ell(g, z') \\ V_\ell(g, z') \\ W_\ell(g, z') \\ X_\ell(g, z') \end{bmatrix}$$

NOTE: The  $\ell$ -sequences pertaining to the representations of the double group  $D_{3d}^{(d)}$ . The notation is explained in Appendix B.



increment of  $\pm 3$ . Equation (3-1) is valid for each spinor component individually. When  $\sin[6\Phi_0(g)] \neq 0$  the  $\ell$ -periodicity relationship becomes more complex, however, this situation does not arise in our example (Section 5 and I).

The comparison of the multipole content of the wave function (i.e., the allowed  $\ell$  values) with spin (Tables 3-1, 3-2) with the corresponding tables in the no-spin case (Tables 3-2, 3-3 in I) is instructive. By matching the allowed  $\ell$ -value sequences, it is possible to infer the representations admixed by the SO interaction. Consider first a  $\Lambda$ -point, i.e., Table 4-1 and Table 3-2 in I. From the comparison we conclude that the spinless  $\Lambda_1, \Lambda_2$  representations are admixed with the  $\Lambda_3$  representation to yield the  $\Lambda_6$  spin representation. On the other hand, the spin representations  $\Lambda_4, \Lambda_5$  result from the splitting the degeneracy of the spinless  $\Lambda_3$  representation by the SO interaction. At the L-point, comparing Table 3-2 with Table 3-3 in I implies that the SO interaction mixes  $L_1, L_2$ , with  $L_3$  (and  $L_1', L_2'$ , with  $L_3'$ ) to give the spin representation  $L_6^+$  (or  $L_6^-$ ).

Consider now the SO vector form factor  $\vec{f}(\vec{r}')$ , Equation (2-11). By comparing it to Equation (2-8), it follows that  $\vec{f}(\vec{r}') = \vec{\nabla}' V(\vec{r}')$  where  $V(\vec{r}')$  transforms as a scalar under the point group transformations. Since  $V(\vec{r}')$  has the multipole expansion Equation (1-1) with  $\ell = 3m, m = 0, \pm 1, \pm 2, \dots$ , and

$$\begin{aligned}\frac{\partial}{\partial x'} &= \cos\phi \frac{\partial}{\partial \rho} - \frac{\sin\phi}{\rho} \frac{\partial}{\partial \phi} \\ \frac{\partial}{\partial y'} &= \sin\phi \frac{\partial}{\partial \rho} + \frac{\cos\phi}{\rho} \frac{\partial}{\partial \phi} \\ \frac{\partial}{\partial z'} &= \frac{\partial}{\partial z'}\end{aligned}\tag{3-3}$$

it follows from the Bessel functions properties<sup>4</sup> that the only SO non-vanishing components are

$$\begin{aligned}f_{3m+1}^{(x')} (g_Q, z') + i f_{3m+1}^{(y')} (g_Q, z') &= -g_Q v_{3m} (g_Q, z') \\ f_{3m-1}^{(x')} (g_Q, z') - i f_{3m-1}^{(y')} (g_Q, z') &= g_Q v_{3m} (g_Q, z') \\ f_{3m}^{(z')} (g_Q, z') &= \frac{\partial}{\partial z'} v_{3m} (g_Q, z') \\ m &= 0, \pm 1, \pm 2, \dots\end{aligned}\tag{3-4}$$

where  $\vec{f}_\ell(g_Q, z') \equiv (f_\ell^{(x')}(g_Q, z'), f_\ell^{(y')}(g_Q, z'), f_\ell^{(z')}(g_Q, z'))$  and  $v_{3m}(g_Q, z')$  are the multipoles of  $V(\vec{r})$ .

Eliminating  $V_{3m}(g_Q, z')$  from Equation (3-4) yields general symmetry relations for the  $S_0$  vector form factor:

$$f_{3m+1}^{(x')} (g_Q, z') = - f_{3m-1}^{(x')} (g_Q, z') = i f_{3m+1}^{(y')} (g_Q, z')$$

$$f_{3m+1}^{(y')} (g_Q, z') = f_{3m-1}^{(y')} (g_Q, z') = i f_{3m-1}^{(x')} (g_Q, z')$$

$$\text{for } m = 0, \pm 1, \pm 2, \dots \quad (3-5)$$

When the  $\ell$ -sequence of Equation (3-5) is compared to Table 3.3 in I, it follows that  $f^{(x')}(\vec{z}')$ ,  $f^{(y')}(\vec{z}')$  transform as  $L_3'$  while  $f^{(z')}(\vec{z}')$  transforms as the  $L_2'$  representations of  $D_{3d}$ .

## SECTION 4

## THE MULTIPOLES WAVE EQUATIONS

In this section the wave equation for the multipoles<sup>1</sup> is generalized to include the spin degrees of freedom and the SO interaction. We follow the method in I, i.e., first the interaction terms are transcribed to a product form and then the decomposition theorem is applied.

In the primed coordinates, the Schrodinger equation with spin-orbit interaction is

$$[-\vec{\nabla}'^2 + \frac{2m_0}{\hbar^2} E_n(\vec{k}) - \frac{2m_0}{\hbar^2} v(\vec{r}') - \frac{2m_0}{\hbar^2} (\hat{V}_{SO}(\vec{r}'))](\psi_{n\vec{k}}(\vec{r}')) = 0 \quad (4-1)$$

where  $(\hat{V}_{SO}(\vec{r}'))$  is the SO interaction and  $m_0$  is the effective mass, chosen to be the free electron mass. Inserting the wave function multipole expansion Equation (2-6) into Equation (4-1), projecting on  $e^{i\ell\phi}$  and factoring out the Bessel functions, we obtain:

$$\sum_{\sigma=\pm 1} \left\{ \left[ -g_0^2 + \frac{2m_0}{\hbar^2} E_n(\vec{k}) + \frac{d^2}{dz'^2} \right] \psi_{\ell}^{(\sigma)}(g_0 z') - \frac{2m_0}{\hbar^2} X_{\ell}^{(\sigma)}(g_0, z') - \frac{2m_0}{\hbar^2} (Y_{\ell}^{(\sigma)}(g_0, z')) \right\} (\chi'(\sigma)) = 0 \quad (4-2)$$

In Equation (4-2) the  $X_{\ell}^{(\sigma)}$  and  $(Y_{\ell}^{(\sigma)})$  terms originate from the products " $v(r')\psi(r')$ " and " $(V_{SO}(\vec{r}') \psi(\vec{r}'))$ " in the Schrodinger Equation, respectively. The former has been discussed extensively in I. The latter is new. Specifically, the goal is to express  $(Y_{\ell}^{(\sigma)}(g_0, z'))$  in terms of multipoles pertaining to the SO form factor and the wave function. Details are given in Appendix C; the rest of the details are readily carried over from I. These steps yields the multipoles wave equation.

$$\begin{aligned}
 & \left[ -g_0^2 + \frac{2m_0}{\hbar^2} E_n(\vec{k}) + \frac{d^2}{dz'^2} \right] \begin{bmatrix} \psi_{\ell}^{(1)}(g_0, z') \\ \psi_{\ell}^{(-1)}(g_0, z') \end{bmatrix} + \\
 & + \sum_{g_P, g_F} \sum_{m=-2}^3 A_{\ell, m}(g_0, g_P, g_F) \left\{ -\frac{2m_0}{\hbar^2} \begin{bmatrix} v_m(g_P, z') & 0 \\ 0 & v_m(g_P, z') \end{bmatrix} \begin{bmatrix} \psi_{\ell-m}^{(1)}(g_F, z') \\ \psi_{\ell-m}^{(-1)}(g_F, z') \end{bmatrix} \right. \\
 & \quad - \frac{2m_0}{\hbar^2} \begin{bmatrix} 0 & f_m^{(-)}(g_P, z') \\ -f_m^{(+)}(g_P, z') & 0 \end{bmatrix} \begin{bmatrix} \frac{\partial}{\partial z'} \psi_{\ell-m}^{(1)}(g_F, z') \\ \frac{\partial}{\partial z'} \psi_{\ell-m}^{(-1)}(g_F, z') \end{bmatrix} \\
 & \quad - \frac{2m_0}{\hbar^2} \frac{g_F}{2} \begin{bmatrix} f_m^{(-)}(g_P, z') & 0 \\ -2f_m^{(z')} (g_P, z') & -f_m^{(-)}(g_P, z') \end{bmatrix} \begin{bmatrix} \psi_{\ell-m-1}^{(1)}(g_F, z') \\ \psi_{\ell-m-1}^{(-1)}(g_F, z') \end{bmatrix} \\
 & \quad \left. - \frac{2m_0}{\hbar^2} \frac{g_F}{2} \begin{bmatrix} f_m^{(+)}(g_P, z') & -2f_m^{(z')} (g_P, z') \\ 0 & f_m^{(+)}(g_P, z') \end{bmatrix} \begin{bmatrix} \psi_{\ell-m+1}^{(1)}(g_F, z') \\ \psi_{\ell-m+1}^{(-1)}(g_F, z') \end{bmatrix} \right\} = 0 \quad (4-3a)
 \end{aligned}$$

The symbols in Equation (4-3) denote the following: The band energy is denoted by  $E_n(k')$ , the  $\psi_{\ell}^{(\pm 1)}(g_F, z')$  are the two spin components multipoles of the wave function (Equation (2-6)),  $v_m(g_P, z')$  are the multipoles of  $v(\vec{r}')$  - the central potential (Equation (4-1)), the SO vector multipoles  $f_m^{(\pm)}(g_P, z')$  and  $f_m^{(z')} (g_P, z')$  are defined in Equations (2-14), (3-4) and

$$f_{\ell}^{(\pm)}(g_P, z') = f_{\ell}^{(x')} (g_P, z') \pm i f_{\ell}^{(y')} (g_P, z') \quad (4-3b)$$

and the geometrical  $A_{\ell, m}(g_0, g_P, g_F)$ -coefficients have been introduced and discussed in I. The selection rules for  $\ell$ ,  $m$ ,  $g_F$  and  $g_P$  are incorporated into the A-coefficients. The boundary conditions for the wave function multipoles are derived from the Bloch theorem in the [111] direction

$$\psi_{\ell}^{(\sigma)}(g_F, z' + a^*) = e^{ik'a^*} \psi_{\ell}^{(\sigma)}(g_F, z') \quad (4-3c)$$

where  $k', a^*$  are defined in Equation (2-5).

The single variable wave equations, Equation (4-3), is the central result of this work. The band symmetry is specified by the selected  $\ell$ -sequence according to Tables 3-1 and 3-2. Note that the  $\ell$ -sequence for  $\psi_{\ell}^{(\sigma)}(g_F, z')$  depends on  $\sigma$ , the spin projection. The selected  $g$  values, in ascending order (Table 1-1), are controlled by considerations of convergence and available computing capacity.

An interesting feature of Equation (4-3) is the appearance of first derivative ( $\partial/\partial z'$ ) terms. They originate from the  $z'$  derivative terms in  $\vec{L} \cdot \vec{S}$ . The SO interaction in Equation (4-5) has both diagonal and off-diagonal terms in  $\sigma$ . The former shift the no-spin bands as determined by the central potential  $v_m(g_p, z')$  while the latter admix or split the no-spin bands. While in Equation (4-5) both terms are controlled by the same spin interaction, we will argue in the next section that in the context of a phenomenological approach these two types of terms should be parametrized separately.

## SECTION 5

BAND STRUCTURE OF PbSe IN THE  $\Gamma$ -L ([111]) DIRECTION

To demonstrate the viability of the present method, we calculate in this section the low bands of PbSe along the  $\Gamma$ -L direction. This example has been analyzed in I in the absence of SO interaction. The analysis serves a dual purpose: to examine the implementation of the wave equation (4-3) and to demonstrate the type of physical insight the present approach provides. Since the convergence of the multipole expansion has been demonstrated in I, we consider here only the SO effects. To keep the discussion focused, the section is subdivided according to the various aspects of the analysis.

## THE SPIN-ORBIT INTERACTION

We discuss first Equation (4-5) in the context of the  $L_6^+(\Lambda_6)$  and  $L_{4,5}^+(\Lambda_{4,5})$  symmetries. The  $\ell$ -values for which the SO form factor Equation (2-14) does not vanish, given the symmetry relations Equation (3-5), are shown in Table 5-1. The wave-function  $\ell$ -sequences for the above symmetries are given in Tables 3-1, 3-2. Combining these two  $\ell$ -constraints yields the wave equation block structure in  $\sigma$ , the spin projection, displayed in Table 5-2: For the  $L_6^+(\Lambda_6)$  bands, the SO terms occur in one diagonal block ( $\ell = 3m+1$ ) and the off diagonal blocks, Table (5-2a). On the other hand, for the  $L_{4,5}^+(\Lambda_{4,5})$  bands only the diagonal blocks ( $\ell = 3m\pm 1$ ) have SO terms, Table (5-2b). This structure has a physical interpretation recalling that the  $\ell = 3m$  blocks are associated with s-waves (and higher even waves) whereas the  $\ell = 3m\pm 1$  blocks with p-waves (and higher odd waves). Thus the diagonal SO terms in the  $\ell = 3m\pm 1$  describe the p-wave SO interaction while the off diagonal SO terms describe the s-p SO mixing. Since the  $s_{1/2}$  and  $p_{1/2}$  interactions are, in general, quite different,<sup>11</sup> it is expected that these two types of terms have different strengths.

The parametrization of the SO interaction depends on the specifics of the material. Since PbSe has two atoms in the unit cell, the SO form factor  $f_j(|\vec{r}-\vec{r}_j|)$ , Equation (2-11) and Appendix D, requires four parameters: the two strengths and two ranges of the atomic SO interactions. The SO ranges are taken to be that of Pb and Se atomic cores: The Pb core (Xe  $4f^{14} 5d^{10}$ ) is approximately that of Ar and the Se core (Au  $3d^{10}$ ) is approximately that of Cu. The core radii values are given in Table 5-3. The radial dependence is taken to be a gaussian. A box form factor gives similar results (Appendix D).

TABLE 5-1. SYMMETRY PROPERTIES OF THE SPIN-ORBIT FORM FACTOR  $\vec{f}_m(g_P, z')$

m	$f_m^{(+)}(g_P, z')^{(a)}$	$f_m^{(-)}(g_P, z')^{(a)}$	$f_m^{(z')}(g_P, z')^{(b)}$
-2	$B(z')$	0	0
-1	0	$A(z')$	0
0	0	0	$C(z')$
1	$-A(z')$	0	0
2	0	$B(z')$	0
3	0	0	$D(z')$

(a)  $A(-z') = A(z')$ ,  $B(-z') = -B(z')$

(b)  $C(-z') = -C(z')$ ,  $D(-z') = D(z')$

NOTE: The non-vanishing components and symmetries of the SO form factor (Equation (3-4), (4-3b)).

TABLE 5-2. BLOCK STRUCTURE OF WAVE EQUATIONS (4-3)

$$\begin{array}{cc}
 \begin{array}{c} \sigma=-1 \\ (3m+1) \end{array} & \begin{array}{c} \sigma=-1 \\ (3m+1) \end{array} \\
 \begin{array}{c} \sigma=-1 \\ (3m+1) \end{array} & \begin{array}{c} \sigma=+1 \\ (3m) \end{array}
 \end{array}
 \left[ \begin{array}{cc}
 v_m(g_P, z') + f_m^{(\pm)}(g_P, z') & f_m^{(\pm)}(g_P, z') \frac{\partial}{\partial z'} + f_m^{(z')} (g_P, z') \\
 f_m^{(\pm)}(g_P, z') \frac{\partial}{\partial z'} + f_m^{(z')} (g_P, z') & v_m(g_P, z')
 \end{array} \right]$$

 (a):  $L_6^{\pm}(\Lambda_6)$  representations

$$\begin{array}{cc}
 \begin{array}{c} \sigma=-1 \\ (3m+1) \end{array} & \begin{array}{c} \sigma=-1 \\ (3m+1) \end{array} \\
 \begin{array}{c} \sigma=-1 \\ (3m+1) \end{array} & \begin{array}{c} \sigma=+1 \\ (3m-1) \end{array}
 \end{array}
 \left[ \begin{array}{cc}
 v_m(g_P, z') + f_m^{(\pm)}(g_P, z') & 0 \\
 0 & v_m(g_P, z') + f_m^{(\mp)}(g_P, z')
 \end{array} \right]$$

 (b):  $L_{4,5}^{\pm}(\Lambda_{4,5})$  representations

NOTE: Schematic block structure of the wave functions Equation (4-3) for the  $L_6^{\pm}(\Lambda_6)$  and  $L_{4,5}^{\pm}(\Lambda_{4,5})$  bands. The  $\sigma$  and  $l$ -sequence indices are explicitly indicated.



TABLE 5-3. SPIN-ORBIT PARAMETERS

$$\hat{H}_{SO} = s(\hat{\vec{\sigma}} \cdot \hat{\vec{\ell}})$$

	$\lambda_{Se}$ [eV]	$\lambda_{Pb}$ [eV]	$r(Pb)(\text{\AA})$	$r(Se)(\text{\AA})$
<u>REFERENCE</u>				
J. C. Philips <sup>(a)</sup>	.16	.66		
H. J. Zeiger and G. W. Pratt <sup>(b)</sup>	.14	.45		
This Work	.14	.56	1.45	1.16

(a) We use  $\lambda = .33*\Delta_A$  where  $\Delta_A$  is a spin-orbit splitting of Atom A, Equation (7-28) in Reference 3, p.179.

(b) We use Equation (3-61) in Reference 7 for the Atomic Spin-orbit Strengths.

NOTE: The spin orbit parameters, see Appendix D. The s and r parameters denote the atomic SO strength and range parameters, respectively.

The SO strengths are chosen as follows. The ratio of the Pb and Se SO strengths is taken from atomic data (see Table 5-3). This ratio is roughly 3.-4. and is kept fixed. The overall SO strengths, however, are adjustable parameters. According to the above remark, the diagonal SO blocks (in Table 5-2) pertain to the p-wave whereas the off diagonal SO blocks pertain to s-p SO mixing. Consequently we introduce two dimensionless SO scale parameters:  $S_{ND}$ , a nondiagonal SO parameter and  $S_D$  an diagonal SO parameter such that

$$A(Pb) = \begin{bmatrix} S_D \\ S_{ND} \end{bmatrix} \lambda_{Pb}, \quad A(Se) = \begin{bmatrix} S_D \\ S_{ND} \end{bmatrix} \lambda_{Se} \quad (5-1)$$

where  $\lambda_{Pb}$ ,  $\lambda_{Se}$  are the "atomic" spin orbit strengths of Pb and Se, Table 5-3, and  $A(Pb)$ ,  $A(Se)$  are the overall atomic SO strengths (see Appendix D). The signs and magnitudes of  $S_{ND}$ ,  $S_D$  are determined by fitting two measured band gaps (see the next subsection). Consider the  $L_6^+$  bands (Table (5-2a)). The "v" terms in the  $\ell=3m$  block correspond to the  $s_{1/2}$  potential. By the same token, the "v +  $f^\pm$ " terms in the  $\ell=3m+1$  block correspond to the  $p_{1/2}$  potential. Since the latter is less positive than the former,<sup>11</sup> we can expect  $S_D < 0$  to make " $f^\pm$ " negative. Strictly speaking, the wave equation, Equation (4-3), implies that  $S_{ND} = S_D$ . However if  $S_{ND} \neq S_D$ , it is reasonable to expect them to share the same sign. Thus, heuristically, we expect both  $S_{ND}$  and  $S_D$  are negative.

#### RESULTS FOR PbSe ALONG THE [111] DIRECTION

The four relevant bands near the Fermi level are apparent from Figure 5-1a.<sup>1</sup> These particular no-spin bands are calculated using an eight-multipole basis, which is a computational compromise between a fully convergent basis (12 multipoles) and our computing capacity. A consequence of the eight-multipoles basis choice is that the no-spin bands are not adequately described for  $K \leq 5$  (Equation (2-5)), i.e., for the lower half of the  $\Gamma$ -L line.

At the L-point, the SO interaction admixes the  $(L_3, L_1)$  and the  $(L_3', L_2')$  bands, respectively. This is evident from comparing the  $\ell$ -sequences for the  $L_6^+$  bands (Table 3-2) with those of  $L_3$  and  $L_1$  bands, (see I). Consequently, given the particular arrangement of the  $L_3, L_1, L_2, L_3'$  bands in Figure 5-1a, it is expected that the band gap  $\Delta E_G \approx E(L_2) - E(L_1)$  will be reduced by the SO interaction. This trend is demonstrated in Table 5-4 and Figure 5-2 for the near- $E_F$   $L_6^+$  bands. Consider first the limit of  $S_{ND} = 0$ . From Table 5-2 it follows that in this case only the p-wave ( $\ell=3m+1$ ) blocks are modified. This is evident from the first two columns of Table 5-4 where the  $L_3, L_3'$  bands (the two outermost  $L_6^+$  bands) move while the  $L_1, L_2$  bands (the two innermost  $L_6^+$  bands) do not. Positive  $S_D$  tends to cluster the bands while, conversely,  $S_D < 0$  fans out the bands. In the other limit, i.e.,  $S_D = 0$ , Table 5-2a implies that only off-diagonal s-p mixing blocks exist. In this case the band gap is reduced as expected and all bands move down. This statement is true for both positive and negative  $S_{ND}$ . When both  $S_{ND}$  and  $S_D$  are nonzero, a combination of the above two effects is observed. In particular, when  $S_{ND}$  and  $S_D$  have the same sign, then the bands either cluster together for  $S_{ND}, S_D > 0$  or fan out

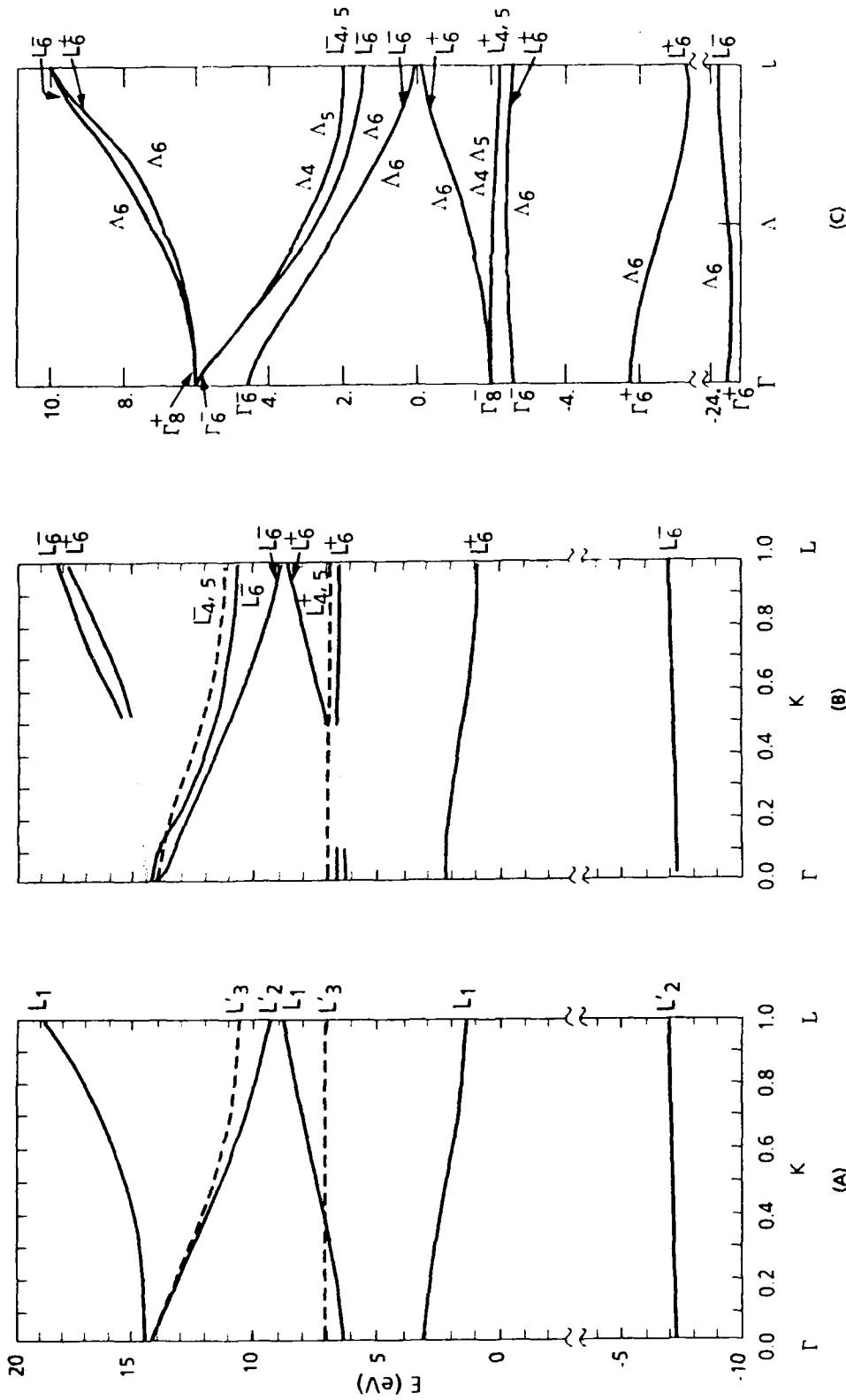
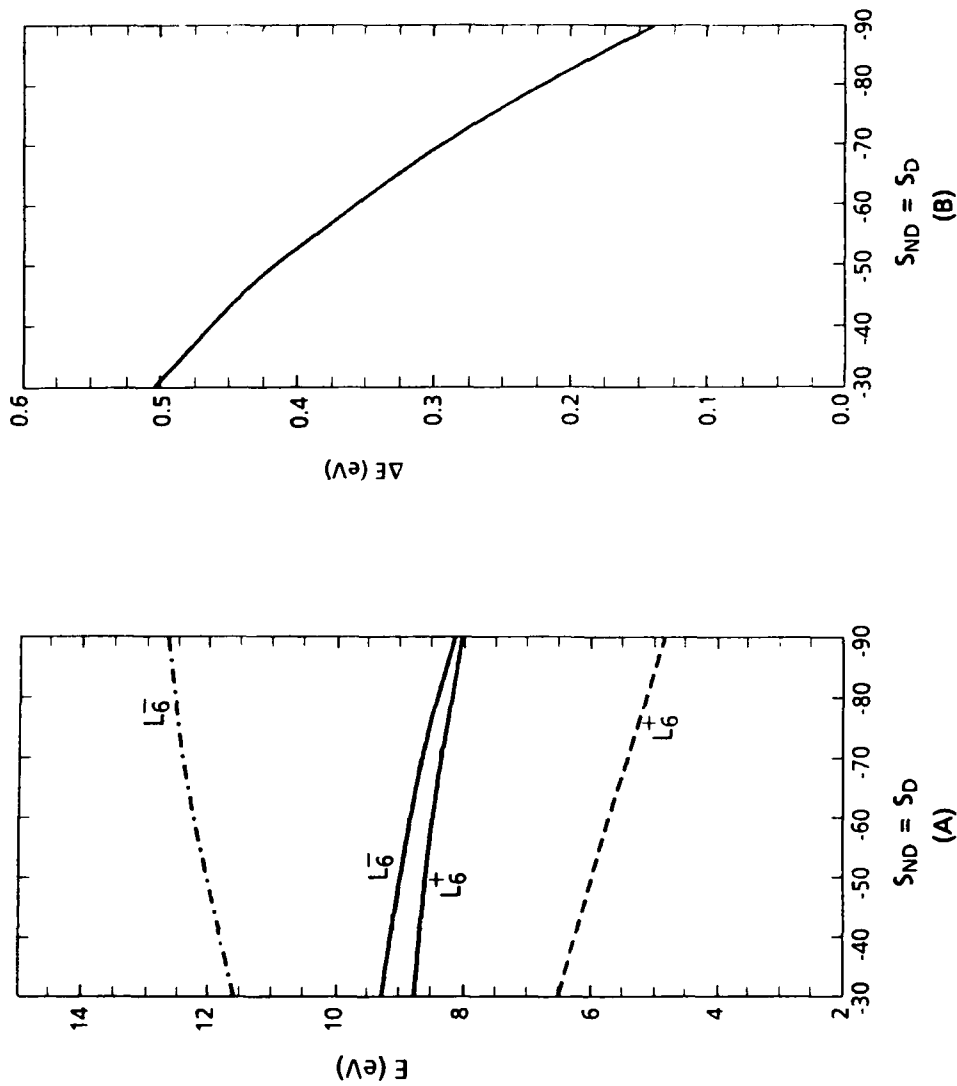


FIGURE 5-1. CALCULATED BAND STRUCTURES OF PbSe ALONG THE  $\Gamma$ -L DIRECTION

TABLE 5-4. BAND ENERGY DEPENDENCE ON SPIN-ORBIT PARAMETERS AT THE L-POINT  $L_6^{\pm}$ 

	$S_{ND}$	0	0	0	$\pm 30.$	30.	-30.
	$S_D$	0	-20.	20	0	30.	-30.
Band Symmetry							
$L_6^-$	10.718	11.436 $\uparrow$	9.965 $\downarrow$	10.573 $\uparrow$	9.977 $\downarrow$	11.670 $\uparrow$	
$L_6^-$	9.424	9.424	9.424	9.312 $\downarrow$	9.439 $\uparrow$	9.297 $\downarrow$	
$L_6^+$	8.853	8.853	8.853	8.830 $\downarrow$	9.093 $\downarrow$	8.792 $\downarrow$	
$L_6^+$	7.180	6.816 $\downarrow$	7.503 $\uparrow$	7.053 $\downarrow$	7.501 $\uparrow$	6.540 $\downarrow$	
$\Delta E$	0.571	0.571	0.571	0.482	0.366	.505	

NOTE: The dependence of near- $E_F$  PbSe band energies, at the L-point, on the two spin-orbit parameters, Equation (5-1). The trend of the band movement (in energy) is indicated by an arrow and the band gap,  $\Delta E$ . All energies are given in eV.



Note: Figure 5-2(A) shows the four important bands; Figure 5-2(B) shows the corresponding band gap  $\Delta E$ .

FIGURE 5-2. THE DEPENDENCE OF NEAR-EF BANDS AT THE L-POINT ON THE SPIN-ORBIT STRENGTH  $S_D = S_D < 0$

for  $S_{ND}, S_D < 0$  and the band gap is reduced. Figures 5-2a and 5-2b demonstrate the trend for the physically relevant case when  $S_{ND}, S_D < 0$ . Note that a sufficiently strong SO interaction reduces the band gap to the point of "band inversion," and beyond. This effect of the SO interaction is well known in narrow gap semiconductors, such as in the IV-VI.

Figures 5-1b and 5-1c show the calculated lowest ten bands and the corresponding results from Kohn's work.<sup>12</sup> Numerical details of the calculation are given in Appendix E. We choose the SO parameters as  $S_{ND} = -60.$ ,  $S_D = -15$  to approximately reproduce two experimental band gaps at the L-point: the smallest gap ( $E(L_6^-) - E(L_6^+)$ ) and a secondary gap between the two adjacent  $L_6^+$  bands. As Figures 5-1b and 5-1c show, this choice reproduces quite well all the bands and relative spacings at the L-point and down to about the mid-point of the  $\Gamma$ -L line. For smaller K values, some bands are missing, and not all bands are in the correct order (Figure 5-1c is the correct band structure). We understand these deficiencies as numerical artifacts that originate from the eight-multipoles no-spin base choice. As Figure 5-1a shows, for  $K \approx .5$  we have a spurious crossing of the  $L_1$  and  $L_3$  bands. This crossing creates a wrong sequence for two bands at the  $\Gamma$ -point. Obviously, the SO mixing cannot rectify this deficiency; hence, the wrong sequence at the  $\Gamma$ -point (Figure 5-1b). In addition, the  $(L_1, L_3)$  crossing generates a degeneracy of equal-parity bands. For numerical reasons, the code does not deal correctly with a situation of several, closely spaced and mixed bands. This is the reason for the missing of a few bands for limited range of K values. The same situation occurs at  $E \approx 14$  eV, where again two closely spaced bands occur.

From the comparison of Figures (5-1a) through (5-1c), we conclude that, whenever the no-spin basis is adequate (i.e.,  $K \approx .5$  in our case), the bands calculated by the present method compare well with the correct band structure. Conversely, whenever the no-spin basis is deficient (i.e.,  $K \approx .5$  in our case), the calculated bands with the SO interaction are deficient. This outcome obviously suggests the choice of the fully convergent no-spin base as a starting point, i.e., the 12 multipoles<sup>1</sup> (valid throughout the  $\Gamma$ -L line) rather than the eight-multipoles basis used here. Such a calculation, however, is beyond our present numerical capacity.

## SECTION 6

### SUMMARY AND DISCUSSION

We have generalized the cylindrical multipole approach to band structure to include spin degrees of freedom and the SO interaction. The ensuing one-dimensional set of wave equations is solved for the test case of PbSe in the [111] direction. The results are compared with the band structure calculated by an entirely different method.<sup>13</sup>

The combination of the formalism and test calculations demonstrates advantages and limitations of the present approach. We have shown that the SO interaction is accommodated naturally in the present formalism. Another advantage of the present representation is that it obviates the band symmetries which are admixed by the SO interaction. Thus, for instance, we can readily understand the band-gap reduction at the L-point by the SO interaction and the tendency to band inversion for sufficient strong SO interaction. The calculated PbSe band structure in the [111] direction yields the correct sequence and spacings at and around the L-point, where the Fermi-level lies.

On the other hand, the method in its present form does not reproduce, degenerate, or quasi-degenerate bands. At the  $\Gamma$ -point this problem can be possibly alleviated provided the  $\Gamma$ -point symmetries can be introduced. At other points on the  $\Gamma$ -L line, a fully convergent no-spin basis avoid incorrect band ordering.

# REFERENCES

1. Agassi, D., and Restorff, J. B., Pseudopotential Band Calculations Along a High-Symmetry Axis: Part I--Central Potential and the [111] Direction, NAVSWC TR 91-324, 15 Jun 1991.
2. Nimtz, G., and Schlicht, B., in Narrow Gap Semiconductors, Springer Tracts in Modern Physics, Vol. 98, Springer-Verlag, Berlin, 1985, "Physics and Chemistry of II-VI Compounds," Aven, M., and Prener, J. S., Editors, North Holland, Amsterdam, 1962.
3. Philips, J. C., Bonds and Bands in Semiconductors, Academic Press, New York, 1973, p. 123.
4. Abramowitz, M., and Stegun, I. A., Handbook of Mathematical Functions, National Bureau of Standards, Applied Mathematics, Series 55, Washington, 1964, Ch. 9.
5. McKelvey, J. P., Solid State and Semiconductor Physics, Harper and Row, New York, and John Weatherhill, Inc., Tokyo, 1969, pp. 212-217.
6. Morgan, D. J., Solid State Theory, Landsberg, P. T., Editor, Wiley-Interscience, London, 1965, pp. 232-254.
7. Zeiger, H. J., and Pratt, G. W., Magnetic Interactions in Solids, Clarendon Press, Oxford, 1973, Appendix 4.
8. Slater, J. C., Quantum Theory of Molecules and Solids, Vol. 2, McGraw-Hill, New York, 1965, Appendix 9.
9. Jones, H., The Theory of Brillouin Zones and Electronic States in Crystals, North Holland, Amsterdam, 1975, Second Edition, Ch. 7.
10. Dalven, R., Solid State Physics, Vol. 28, Ehrenreich, H., Seitz, F., and Turnbull, D., Editors, Academic Press, New York, 1973.
11. Rabe, K. M., and Joannopoulos, J. D., Phys. Rev., 32, p. 2302, 1985.
12. Kohn, S. E., Yu, R. Y., Petroff, Y., Shen, Y. R., Tsang, Y., and Cohen, M. L., Phys. Rev. B 8, p. 1477, 1973.
13. Landsberg, P. T., Solid State Theory, Landsberg, P. T., Editor, Wiley-Interscience, London, 1969, p. 77.



# APPENDIX A

## IRREDUCIBLE REPRESENTATIONS OF THE DOUBLE GROUPS $C_{3v}^{(d)}$ AND $D_{3d}^{(d)}$

Double groups arise when spatial symmetry operators act on products of the form  $\Psi(\vec{r})(\chi)$  where  $(\chi)$  is a spinor. Since (Equation (2-3))

$$\hat{R} [\Psi(\vec{r})(\chi)] = [\hat{R} \Psi(\vec{r})] [\hat{R}(\chi)] \quad (A-1)$$

the matrices of  $\hat{R}$  in this basis form a group, termed the "double group." The term reflects the fact that  $[\hat{R}(\chi)]$  changes sign when any Euler angle is changed by  $2\pi$ . Hence to every rotation  $\hat{R}$  correspond two matrices  $(R)$  and  $(\bar{R})$  such that  $(\bar{R}) = -(R)$ . Thus the order of a double group is twice that of the original group. <sup>A-1, A-2</sup>

For the sake of completeness we quote again <sup>A-3</sup> the cylindrical coordinates realization of the groups  $C_{3v}$  and  $D_{3d}$ :

- 
- A-1 Morgan, D. J., Solid State Theory, Landsberg, P. T., Ed., Wiley-Interscience, London 1965, pp. 232-254.
  - A-2 Slater, J. C., Quantum Theory of Molecules and Solids, Vol. 2, McGraw-Hill, New York, NY, 1965, Appendix 9.
  - A-3 Agassi, D. and Restorff, J. B., Pseudopotential Band Calculations Along a High-Symmetry Axis: Part I--Central Potential and the [111] Direction, NAVSWC TR 91-324, 15 Jun 1991).

$C_{3v}$	$D_{3d}$
$X_0 \Psi(\phi) = \Psi(\phi)$	$X_0 \Psi(\phi, z) = \Psi(\phi, z)$
$X_{\pm 1} \Psi(\phi) = \Psi(\phi \pm 2\pi/3)$	$X_{\pm 1} \Psi(\phi, z) = \Psi(\phi \pm \pi/3, -z)$
$Y_0 \Psi(\phi) = \Psi(-\phi)$	$X_{\pm 2} \Psi(\phi, z) = \Psi(\phi \pm 2\pi/3, z)$
$Y_{\pm 1} \Psi(\phi) = \Psi(-\phi \pm 2\pi/3)$	$X_3 \Psi(\phi, z) = \Psi(\phi + \pi, -z)$
	$Y_0 \Psi(\phi, z) = \Psi(-\phi, z)$
	$Y_{\pm 1} \Psi(\phi, z) = \Psi(-\phi \pm \pi/3, -z)$
	$Y_{\pm 2} \Psi(\phi, z) = \Psi(-\phi \pm 2\pi/3, z)$
	$Y_3 \Psi(\phi, z) = \Psi(-\phi + \pi, -z)$

(A-2)

In Equation (A-2)  $\Psi$  is an arbitrary function and  $\phi, z$  are the cylindrical azimuthal angle and  $z$  coordinate, respectively. Note that  $Y_0$  is a plane reflection and  $X_3$  is the inversion operator with respect to the origin.

According to Equation (A-1), to calculate the double group irreducible representations requires the knowledge of  $R(\chi)$ . This matter is discussed in Reference (A-2) and we bring here only the results. For  $C_{3v}^{(d)}$ , the double group corresponding to  $C_{3v}$ , the results are:

$$\begin{aligned}
 & X_{\pm 1} |\alpha\rangle = \Omega^{\pm 1} |\alpha\rangle, \quad X_{\pm 1} |\beta\rangle = \Omega^{\mp 1} |\beta\rangle \\
 C_{3v}^{(d)}: & Y_0 |\alpha\rangle = |\beta\rangle, \quad Y_0 |\beta\rangle = -|\alpha\rangle \\
 & Y_{\pm 1} |\alpha\rangle = \Omega^{\pm 1} |\alpha\rangle, \quad Y_{\pm 1} |\beta\rangle = -\Omega^{\mp 1} |\beta\rangle \\
 & \Omega = e^{i\pi/3}
 \end{aligned}
 \tag{A-3}$$

where in Equation (A-3) and throughout this appendix,  $(\alpha)$  and  $(\beta)$  denote "spin up" and "spin down" spinors, respectively.

The representations  $\hat{\Gamma}$  are defined according to

$$\hat{R} |i\rangle = \sum_j |j\rangle \langle j | \hat{R} | i \rangle
 \tag{A-4}$$

where  $|i\rangle$  is an appropriate basis state. For the  $C_{3v}^{(d)}$  irreducible spin representations, we choose the following basis:

$$\begin{aligned}
 \Lambda_4: \quad |1\rangle &= e^{i\phi}|\alpha\rangle + i e^{-i\phi}|\beta\rangle \\
 \Lambda_5: \quad |1\rangle &= e^{i\phi}|\alpha\rangle - i e^{-i\phi}|\beta\rangle \\
 \Lambda_6: \quad |1\rangle &= |\alpha\rangle, \quad |2\rangle = |\beta\rangle
 \end{aligned} \tag{A-5}$$

The ensuing irreducible representations are given in Table A-1.

The group  $D_{3d}^{(d)}$ , the double group corresponding to  $D_{3d}$ , contains in addition to the operators Equation (A-3) the space inversion and a  $\pm\pi/3$  rotation of  $\phi$ . The former does not effect spinors. Using the techniques of Reference A-2, we obtain:

$$\begin{aligned}
 X_{\pm 1}|\alpha\rangle &= \Omega^{\mp 1}|\alpha\rangle, \quad X_{\pm 1}|\beta\rangle = \Omega^{\pm 1}|\beta\rangle \\
 D_{3d}^{(d)}: \quad X_3|\alpha\rangle &= |\alpha\rangle, \quad X_3|\beta\rangle = |\beta\rangle \\
 Y_{\pm 1}|\alpha\rangle &= \Omega^{\mp 1}|\beta\rangle, \quad Y_{\pm 1}|\beta\rangle = -\Omega^{\pm 1}|\alpha\rangle \\
 Y_0|\alpha\rangle &= |\beta\rangle, \quad Y_0|\beta\rangle = -|\alpha\rangle
 \end{aligned} \tag{A-6}$$

The irreducible representations in Table A-2 are obtained from Equation (A-6) and the following basis:

$$\begin{aligned}
 L_4^+: \quad |1\rangle &= [e^{i\phi}|\alpha\rangle - i e^{-i\phi}|\beta\rangle] U(z), \quad U(z) = -U(-z) \\
 L_5^+: \quad |1\rangle &= [e^{i\phi}|\alpha\rangle + i e^{-i\phi}|\beta\rangle] U(z), \quad U(z) = -U(-z) \\
 L_4^-: \quad |1\rangle &= [e^{i\phi}|\alpha\rangle - i e^{-i\phi}|\beta\rangle] U(z), \quad U(z) = U(-z) \\
 L_5^-: \quad |1\rangle &= [e^{i\phi}|\alpha\rangle + i e^{-i\phi}|\beta\rangle] U(z), \quad U(z) = U(-z) \\
 L_6^+: \quad |1\rangle &= |\alpha\rangle U(z), \quad |2\rangle = |\beta\rangle U(z), \quad U(z) = U(-z) \\
 L_6^-: \quad |1\rangle &= |\alpha\rangle U(z), \quad |2\rangle = |\beta\rangle U(z), \quad U(z) = -U(-z)
 \end{aligned} \tag{A-7}$$

The basis functions Equation (A-5) and (A-7) manifest the spin-projection in the  $z'$  direction, denoted by  $m_j$  in Tables A-1 and A-2.

TABLE A-1. IRREDUCIBLE SPIN REPRESENTATIONS OF  $C_{3v}^{(d)}$ 

REPRESENTATION:	$\Lambda_4$	$\Lambda_5$	$\Lambda_6^{(a)}$
$m_J$ :	$\pm 3/2$	$\pm 3/2$	$\pm 1/2$
OPERATOR			
$X_0$	1	1	$\begin{bmatrix} 1 & 0 \\ 0 & 1 \end{bmatrix}$
$X_{\pm 1}$	-1	-1	$\begin{bmatrix} \Omega^{\pm 1} & 0 \\ 0 & \Omega^{\mp 1} \end{bmatrix}$
$Y_0$ (Plane reflection)	-i	i	$\begin{bmatrix} 0 & -1 \\ 1 & 0 \end{bmatrix}$
$Y_{\pm 1}$	i	-i	$\begin{bmatrix} 0 & -\Omega^{\mp 1} \\ \Omega^{\pm 1} & 0 \end{bmatrix}$

$$\bar{X}_i = -X_i, \quad \bar{Y}_i = -Y_i$$

(a)  $\Omega = e^{i\pi/3}$

NOTE: The irreducible spin representations of the double group  $C_{3v}$ . The group operators are defined in Appendix A. The designation of the spin projection in the z-direction,  $m_J$ , is predicated on the corresponding basis functions, see Appendix A.

TABLE A-2. IRREDUCIBLE SPIN REPRESENTATIONS OF  $D_{3d}^{(d)}$ 

REPRESENTATION:	$L_4^+$	$L_5^+$	$L_4^-$	$L_5^-$	$L_6^+ (a)$	$L_6^- (a)$
$m_J$ :	$\pm 3/2$	$\pm 3/2$	$\pm 3/2$	$\pm 3/2$	$\pm 1/2$	$\pm 1/2$
OPERATOR						
$X_0$	1	1	1	1	$\begin{bmatrix} 1 & 0 \\ 0 & 1 \end{bmatrix}$	$\begin{bmatrix} 1 & 0 \\ 0 & 1 \end{bmatrix}$
$X_{\pm 1}$	-1	-1	1	1	$\begin{bmatrix} \Omega^{\mp 1} & 0 \\ 0 & \Omega^{\pm 1} \end{bmatrix}$	$\begin{bmatrix} -\Omega^{\mp 1} & 0 \\ 0 & -\Omega^{\pm 1} \end{bmatrix}$
$X_{\pm 2}$	-1	-1	-1	-1	$\begin{bmatrix} \Omega^{\pm 1} & 0 \\ 0 & \Omega^{\mp 1} \end{bmatrix}$	$\begin{bmatrix} \Omega^{\pm 1} & 0 \\ 0 & \Omega^{\mp 1} \end{bmatrix}$
$X_3$ (z parity)	1	1	-1	-1	$\begin{bmatrix} 1 & 0 \\ 0 & 1 \end{bmatrix}$	$\begin{bmatrix} -1 & 0 \\ 0 & -1 \end{bmatrix}$
$Y_0$ (Plane reflection)	i	-i	i	-i	$\begin{bmatrix} 0 & -1 \\ 1 & 0 \end{bmatrix}$	$\begin{bmatrix} 0 & -1 \\ 1 & 0 \end{bmatrix}$
$Y_{\pm 1}$	-i	i	i	-i	$\begin{bmatrix} 0 & -\Omega^{\pm 1} \\ \Omega^{\mp 1} & 0 \end{bmatrix}$	$\begin{bmatrix} 0 & \Omega^{\pm 1} \\ -\Omega^{\mp 1} & 0 \end{bmatrix}$
$Y_{\pm 2}$	-i	i	-i	i	$\begin{bmatrix} 0 & -\Omega^{\mp 1} \\ \Omega^{\pm 1} & 0 \end{bmatrix}$	$\begin{bmatrix} 0 & -\Omega^{\mp 1} \\ \Omega^{\pm 1} & 0 \end{bmatrix}$
$Y_3$	i	-i	-i	i	$\begin{bmatrix} 0 & -1 \\ 1 & 0 \end{bmatrix}$	$\begin{bmatrix} 0 & 1 \\ -1 & 0 \end{bmatrix}$

$$\bar{X}_i = -X_i, \quad \bar{Y}_i = -Y_i$$

$$(a) \quad \Omega = e^{i\pi/3}$$

(d)

NOTE: The irreducible representations of the double group  $D_{3d}^{(d)}$ . The group operators are defined in Appendix A. The  $m_J$  symbol is the same as in Table 3-1.

## APPENDIX B

### MULTIPOLE CONTENT OF THE $C_{3v}^{(d)}$ AND $D_{3d}^{(d)}$ SPIN REPRESENTATIONS

The allowed  $l$  values for the spin representations of  $C_{3v}^{(d)}$  and the  $D_{3d}^{(d)}$  groups are determined by the method used in Reference B-1. To demonstrate the method, we analyze here the  $\Lambda_6$  representation of the  $C_{3v}^{(d)}$  group. A similar analysis applies to all other representations. The results are given in Tables 3-1 and 3-2 of the main text.

From Table 3-1 it follows that the  $\Lambda_6$  representation is of dimension two. The general multipole expansion of the two basis spinors is

$$\begin{aligned} |1\rangle &= \sum_{l=-\infty}^{\infty} U_l(\rho, z) e^{il\phi} |\alpha\rangle + \sum_{l=-\infty}^{\infty} V_l(\rho, z) e^{il\phi} |\beta\rangle \\ |2\rangle &= \sum_{l=-\infty}^{\infty} W_l(\rho, z) e^{il\phi} |\alpha\rangle + \sum_{l=-\infty}^{\infty} X_l(\rho, z) e^{il\phi} |\beta\rangle \end{aligned} \quad (B-1)$$

where  $(\alpha)$  and  $(\beta)$  are the "up" and "down" spinors respectively. Apply now  $X_{\pm 1}$  and  $Y_0$  to Equation (B-1). Equations (A-1), (A-2) and Table A-1 give:

$$\begin{aligned} X_{\pm 1} |1\rangle &= \Omega^{\pm 1} |1\rangle = \sum_l U_l(\rho, z) e^{il(\phi \pm 2\pi/3)} \Omega^{\pm 1} |\alpha\rangle \\ &+ \sum_l V_l(\rho, z) e^{il(\phi \pm 2\pi/3)} \Omega^{\mp 1} |\beta\rangle \end{aligned} \quad (B-2)$$

---

B-1 Agassi, D. and Restorff, J. B., Pseudopotential Band Calculations Along a High-Symmetry Axis: Part I--Central Potential and the [111] Direction, NAVSWC TR 91-324, 15 Jun 1991.

$$\begin{aligned}
 X_{\pm 1} |2\rangle &= \Omega^{\mp 1} |2\rangle = \sum_{\ell} W_{\ell}(\rho, z) e^{i\ell(\phi \pm 2\pi/3)} \Omega^{\pm 1} |\alpha\rangle \\
 &+ \sum_{\ell} X_{\ell}(\rho, z) e^{i\ell(\phi \pm 2\pi/3)} \Omega^{\mp 1} |\beta\rangle
 \end{aligned} \tag{B-3}$$

$$Y_0 |1\rangle = |2\rangle = \sum_{\ell} U_{\ell}(\rho, z) e^{-i\ell\phi} |\beta\rangle - \sum_{\ell} V_{\ell}(\rho, z) e^{-i\ell\phi} |\alpha\rangle \tag{B-4}$$

where

$$\Omega = e^{i\pi/3} \tag{B-5}$$

We now equate the spin and  $e^{i\ell\phi}$  components on both sides of Equations (B-2 -B-4). Consider first Equation (B-2). Equating the  $U_{\ell}(\rho, z)$  components yields

$$U_{\ell}: e^{\pm i\ell 2\pi/3} = 1 \Rightarrow \ell = 3m, \quad m = 0, \pm 1, \pm 2, \dots \tag{B-6a}$$

and for the  $V_{\ell}(\rho, z)$  components

$$V_{\ell}: e^{\pm i\ell 2\pi/3} \Omega^{\mp 2} = 1 \Rightarrow \ell = 3m+1, \quad m = 0, \pm 1, \pm 2, \dots \tag{B-6b}$$

Similarly,

$$W_{\ell}: e^{\pm i\ell 2\pi/3} \Omega^{\pm 2} = 1 \Rightarrow \ell = 3m-1, \quad m = 0, \pm 1, \pm 2, \dots \tag{B-6c}$$

$$X_{\ell}: e^{\pm i\ell 2\pi/3} = 1 \Rightarrow \ell = 3m, \quad m = 0, \pm 1, \pm 2, \dots \tag{B-6d}$$

To represent Equation (B-6) concisely, we introduce the following representation, also employed in Tables 3-1 and 3-2. Since  $|1\rangle$ ,  $|2\rangle$  in Equation (B-1) are spinors

$$\left[ |\alpha\rangle = \begin{bmatrix} 1 \\ 0 \end{bmatrix}, |\beta\rangle = \begin{bmatrix} 0 \\ 1 \end{bmatrix} \right], \text{ the } U_{\ell}(\rho, z), V_{\ell}(\rho, z) \text{ and } W_{\ell}(\rho, z), X_{\ell}(\rho, z)$$

are the multipole expansion of the "up" components and the "down" component, respectively. Therefore we write Equations (B-6a) and (B-6b) symbolically as

$$|1\rangle = \begin{bmatrix} \ell = 3m \\ \ell = 3m + 1 \end{bmatrix}, \quad m = 0, \pm 1, \pm 2, \dots \tag{B-7}$$

or  $|1\rangle = \begin{bmatrix} 3m \\ 3m + 1 \end{bmatrix}$  as a shorthand notation. Equations (B-6c) and (B-6d) can

similarly be written as

$$|2\rangle = \begin{bmatrix} 3m-1 \\ 3m \end{bmatrix}, \quad m = 0, \pm 1, \pm 2, \dots \quad (\text{B-8})$$

An important property of the multipole expansion is the  $\ell$ -parity, i.e., the phase relation between the  $\ell$  and  $-\ell$  multipoles. This information is derived from Equation (B-4):

$$\begin{aligned} U_{-\ell}(\rho, z) &= X_{\ell}(\rho, z) \\ V_{-\ell}(\rho, z) &= -W_{\ell}(\rho, z) \end{aligned} \quad (\text{B-9})$$

To eliminate the  $\rho$ -dependence from Equation (B-9) recall that, e.g.,

$$U_{\ell}(\rho, z) = \sum_g U_{\ell}(g, z) J_{\ell}(g\rho) \quad (\text{B-10})$$

and  $J_{-\ell}(x) = (-1)^{\ell} J_{\ell}(x)$ . Therefore, inserting Equation (B-10) into Equation (B-9) gives

$$(-1)^{\ell} U_{-\ell}(g, z) = X_{\ell}(g, z) \quad (\text{B-11a})$$

$$-(-1)^{\ell} V_{-\ell}(g, z) = W_{\ell}(g, z) \quad (\text{B-11b})$$

where, from Equation (B-2),  $\ell = 3m$  or  $\ell = 3m+1$ . Equation (B-11) express the  $\ell$ -parity relations. They can be combined into a self evident symbolic matrix notation, see Table 3-3.

The other two spin representations of  $C_{3v}^{(d)}$  are analyzed in the same manner. For the  $D_{3d}^{(d)}$  double group we take the equations generated by  $X_{\pm 1}$ ,  $X_3$ , and  $Y_0$  and employ Equations (A-2) through (A-6) and Table 3-2. The results are given in Table 3-4. Note that a  $D_{3d}^{(d)}$  representation is characterized by the  $z$ -parity, i.e., the phase relation between e.g.,  $U_{\ell}(g, z)$  and  $U_{\ell}(g, -z)$ .

A corollary result is obtained by comparing the  $\ell$ -parity  $\hat{\pi}_{\ell}$  for the allowed  $\ell$  values Tables 3-1 and 3-2. This comparison readily yields the "compatibility relations" between representations pertaining to a  $\Lambda$ -point and the  $L$ -point<sup>B-2</sup>:

B-2 Slater, J. C., Quantum Theory of Molecules and Solids, Vol. 2, McGraw-Hill, New York, NY, 1965, Appendix 9.



$\Lambda$ -point

L-point

$\Lambda_4$

$L_4^+, L_4^-$

$\Lambda_5$

$L_5^+, L_5^-$

$\Lambda_6$

$L_6^+, L_6^-$

(B-13)

## APPENDIX C

## DERIVATION OF EQUATION (4-3)

Straightforward algebra leads (see Reference C-1, Appendix C) to the following expression

$$\begin{aligned}
 (Y_{\ell}^{(\sigma)}(g_0, z')) &= (\hat{\sigma} \cdot \vec{V}_{\ell}^{(\sigma)}) \\
 \vec{V}_{\ell}^{(\sigma)} &= i^{\ell} \sum_{\vec{G}', \vec{L}'} \Psi^{(\sigma)}(\vec{L}') [\vec{f}(\vec{G}') \times (k' \hat{z}' + \vec{L}')] e^{i(G'_z + k' + L'_z)z'} e^{-i\ell\delta(\vec{G}'_T + \vec{L}'_T)} \\
 &\quad |\vec{G}'_T + \vec{L}'_T| = g_0
 \end{aligned} \tag{C-1}$$

In Equation (C-1)  $\hat{z}'$  is the unit vector in the  $z'$ -axis direction,  $\hat{\sigma}$  is the Pauli matrices vector, Equation (2-8), and we limit ourselves to  $\vec{k}'$  vectors parallel to  $\hat{z}'$ . An important feature of Equation (C-1) is that, aside from the  $\hat{\sigma}$  factor, it is a sum of products of two factors pertaining to  $\vec{f}(\vec{r}')$  and  $\Psi_{nk}(\vec{r}')$ , a constrained summation and  $z'$ -dependent exponential. Therefore, according to the multipole decomposition theorem,<sup>C-1</sup>  $V_{\ell}^{(\sigma)}$  can be expressed in terms of products of multipoles pertaining to the two factors.

To carry out this exercise, we first focus on the vector product in Equation (C-1) and introduce the following constructs:

---

C-1 Agassi, D. and Restorff, J. B., Pseudopotential Band Calculations Along a High-Symmetry Axis: Part I--Central Potential and the [111] Direction, NAVSWC TR 91-324, 15 Jun 1991).

$$\Psi_{\ell,x}^{(\sigma)}(g_F, z') = i^\ell \sum_{\vec{L}'} \Psi^{(\sigma)}(\vec{L}') L_x' e^{i(L_z' + k')z'} e^{-i\ell\delta(\vec{L}_T')} \quad |\vec{L}_T'| = g_F$$

$$\Psi_{\ell,y}^{(\sigma)}(g_F, z') = i^\ell \sum_{\vec{L}'} \Psi^{(\sigma)}(\vec{L}') L_y' e^{i(L_z' + k')z'} e^{-i\ell\delta(\vec{L}_T')} \quad |\vec{L}_T'| = g_F$$

$$\Psi_{\ell,z}^{(\sigma)}(g_F, z') = i^\ell \sum_{\vec{L}'} \Psi^{(\sigma)}(\vec{L}') (k' + L_z') e^{i(L_z' + k')z'} e^{-i\ell\delta(\vec{L}_T')} \quad |\vec{L}_T'| = g_F \quad (C-2)$$

By noting that  $(L_x' + iL_y')/g_F = e^{\pm i\delta(\vec{L}')} e^{\pm i\ell\delta(\vec{L}_T')}$  (Reference C-1), these multipoles take the form:

$$\Psi_{\ell,x}^{(\sigma)}(g_F, z') = \frac{ig_F}{2} [\Psi_{\ell-1}^{(\sigma)}(g_F, z') - \Psi_{\ell+1}^{(\sigma)}(g_F, z')]$$

$$\Psi_{\ell,y}^{(\sigma)}(g_F, z') = \frac{g_F}{2} [\Psi_{\ell-1}^{(\sigma)}(g_F, z') + \Psi_{\ell+1}^{(\sigma)}(g_F, z')]$$

$$\Psi_{\ell,z}^{(\sigma)}(g_F, z') = -i \frac{\partial}{\partial z} \Psi_{\ell}^{(\sigma)}(g_F, z') \quad (C-3)$$

Each components of the vector  $\vec{V}_{\ell}^{(\sigma)}$ , Equation (C-1), has the structure of Equation (C-1) in (Reference C-1) provided  $v(\vec{G}')$  is replaced by either  $f_x(\vec{G}')$ ,  $f_y(\vec{G}')$  or  $f_z(\vec{G}')$  (Equation (2-14)), and  $\Psi(\vec{L}')$  is replaced by either  $\Psi^{(\sigma)}(\vec{L}') L_x'$ ,  $\Psi^{(\sigma)}(\vec{L}') L_y'$  or  $\Psi^{(\sigma)}(\vec{L}')(k' + L_z')$ . Therefore, the decomposition theorem (Appendix C, Reference C-1) applies provided  $v_m(g_F, z')$  is replaced by  $\vec{f}_m(g_Q, z')$  (Equation (3-4) in main text) and  $\Psi_{\ell-m}(g_F, z')$  is replaced by Equation (C-3). These steps, and the evaluation of the vector product with  $\vec{\sigma}$  in Equation (C-1) and projection on both  $(\chi(\sigma))$  spinors gives Equation (4-3) of the main text.

## APPENDIX D

## MODELS FOR THE SPIN-ORBIT VECTOR FORM FACTOR

The spin orbit form factor  $\vec{f}(\vec{G}')$  is related to the radial form factor through Equation (2-11) :<sup>D-1</sup>

$$\vec{f}(\vec{G}') = \frac{i}{\Omega} \sum_j e^{i\vec{G}' \cdot \vec{r}_j} \left\{ \vec{\nabla}_{\vec{G}'} \left[ \int_{\Omega} d\vec{r}' e^{i\vec{G}' \cdot (\vec{r}' - \vec{r}_j)} f_j(|\vec{r}' - \vec{r}_j|) \right] \right\} \quad (D-1)$$

In Equation (D-1)  $\Omega$  is the unit cell volume,  $j$  runs over all atoms in the unit cell with coordinates  $\vec{r}_j$  with respect to a chosen origin, and  $f_j(|\vec{r}'|)$  is a phenomenological form factor for the  $j$ -th atom.

The integral in Equation (D-1) should be carried out in the primed coordinates. This is difficult since the integration limits there are awkward. The problem is avoided by transforming the integration to the unprimed coordinates and then applying the  $\vec{\nabla}_{\vec{G}'}$  operator. In the unprimed coordinates the integral in Equation (D-1) takes the form

$$I_j(\vec{G}) = \int_{\Omega} d\vec{r} e^{-i\vec{G} \cdot (\vec{r} - \vec{r}_j)} f_j(|\vec{r} - \vec{r}_j|) \quad (D-2)$$

Therefore, for a separable radial form factor,  $I_j(\vec{G})$  takes a separable form and, hence, easily calculable. The expressions below for a constant  $f_j(|\vec{r} - \vec{r}_j|)$  are easily extended to a separable gaussian.

For a constant radial form factor  $f_j(|\vec{r} - \vec{r}_j|) \equiv A_j$  with a range  $r$ , the integral Equation (D-2) takes the form

$$I_j(\vec{G}) = A_j J_j(G_x) J_j(G_y) J_j(G_z) \quad (D-3)$$

where the integrals  $J_j(G_y)$  depend on whether the atom  $j$  is at the unit cell center (Se) or the eight eighth-atom at the corners of the unit cell (Pb). The former takes the form:

---

D-1 Landsberg, P. T., Solid State Theory, Landsberg, P. T., Ed. Wiley-Interscience, London 1969, p. 77.

$$I_2(G_\gamma) = I_{Se}(G_\gamma) = \int_{-r_{Se}}^{r_{Se}} dt e^{-iG_\gamma t} = Z_2(G_\gamma, r_{Se}) \quad (D-4)$$

where

$$Z_2(G_\gamma, r) = \frac{2 \sin(G_\gamma r)}{G_\gamma}$$

$$Z_2(0, \lambda) = r \quad (D-5)$$

Consider now the integrals  $I_j(G_\gamma)$  pertaining to the Pb atom. For an atom at the  $\vec{r}_1 = (0,0,0)$  corner

$$I_1(G_\gamma) = I_{Pb}^{(1)}(G_\gamma) = \int_0^r dx e^{-iG_\gamma x} = \frac{1}{2} e^{-iG_\gamma r_{Pb}/2} Z_2(G_\gamma/2, r_{Pb}) \quad (D-6)$$

By the same token, the contribution of the  $\vec{r}_2 = (a,0,0)$  corner is

$$I_{Pb}^{(2)}(G_\gamma) = \int_{a-r}^a dx e^{-iG_\gamma(x-a)} = [I_{Pb}^{(1)}(G_\gamma)]^* \quad (D-7)$$

Using similar relations, the  $I_{Pb}(\vec{G})$  contributions from all eight corners are easily evaluated.

We turn now to Equation (D-1) to sum the contribution from all atoms in the unit cell. The tricky parts are the eight Pb contributions located at

$$\vec{r}_1' = (0,0,0), \quad \vec{r}_2' = a \left[ \frac{1}{2} \sqrt{\frac{2}{3}}, -\frac{1}{\sqrt{2}}, \frac{1}{\sqrt{3}} \right]$$

$$\vec{r}_3' = a \left[ \frac{1}{2} \sqrt{\frac{2}{3}}, \frac{1}{\sqrt{2}}, \frac{1}{\sqrt{3}} \right], \quad \vec{r}_4' = a \left[ \sqrt{\frac{2}{3}}, 0, \frac{2}{\sqrt{3}} \right]$$

$$\vec{r}_1' + \vec{r}_8' = \vec{r}_2' + \vec{r}_7' = \vec{r}_3' + \vec{r}_6' = \vec{r}_4' + \vec{r}_5' = \vec{\Delta}' \equiv a^* (0,0,1) \quad (D-8)$$

and  $a^* = a\sqrt{3}$ . With the help of Equation (D-8), the form factor Equation (D-1) takes the form:

$$\vec{f}(\vec{G}') = \frac{1}{\Omega} [ \vec{f}_{Pb}(\vec{G}') + \vec{f}_{Se}(\vec{G}') ] \quad (D-9)$$

where

$$\begin{aligned}
 \vec{f}_{Pb}(\vec{G}') &= 2A_{Pb} e^{-i\vec{G}' \cdot \vec{\Delta}'/2} * \text{Re} \left\{ \right. \\
 &\exp \left[ -i\vec{G}' \cdot (\vec{r}'_1 - \vec{\Delta}'/2) \vec{\nabla}_{\vec{G}'} (I_1(G_x) I_1(G_y) I_1(G_z)) \right] \\
 &+ \exp \left[ -i\vec{G}' \cdot (\vec{r}'_2 - \vec{\Delta}'/2) \vec{\nabla}_{\vec{G}'} (I_1^*(G_x) I_1(G_y) I_1(G_z)) \right] \\
 &+ \exp \left[ -i\vec{G}' \cdot (\vec{r}'_3 - \vec{\Delta}'/2) \vec{\nabla}_{\vec{G}'} (I_1(G_x) I_1^*(G_y) I_1(G_z)) \right] \\
 &+ \exp \left[ -i\vec{G}' \cdot (\vec{r}'_4 - \vec{\Delta}'/2) \vec{\nabla}_{\vec{G}'} (I_1^*(G_x) I_1^*(G_y) I_1(G_z)) \right] \left. \right\} \\
 \vec{f}_{Se}(\vec{G}') &= A_{Se} e^{-i\vec{G}' \cdot \vec{\Delta}'/2} \vec{\nabla}_{\vec{G}'} (I_2(G_x) I_2(G_y) I_2(G_z)) \quad (D-10)
 \end{aligned}$$

To evaluate Equation (D-10), it is necessary to carry out the gradients. Since the gradient transforms like a vector under a rotation, we can immediately write:

$$\left[ \frac{\vec{\partial}}{\partial \vec{G}'_\gamma} \right] = \hat{R} \left[ \frac{\vec{\partial}}{\partial G_\gamma} \right], \quad \gamma = x, y, z \quad (D-11)$$

where  $\hat{R}$  is the transformation from the primed to the unprimed coordinates (Reference D-2, Equation (2-1)). Since both  $I_1(G_\gamma)$  and  $I_2(G_\gamma)$  are given in terms of elementary functions, Equation (D-10) can be evaluated analytically.

For a gaussian form factor, the above analysis remains unchanged except for the expressions for  $I_1(G_\gamma)$ ,  $I_2(G_\gamma)$  which, instead of Equation (D-5), involves the error function.

---

D-2 Agassi, D. and Restorff, J. B., Pseudopotential Band Calculations Along a High-Symmetry Axis: Part I--Central Potential and the [111] Direction, NAVSWC TR 91-324, 15 Jun 1991 (unpublished).

## APPENDIX E

### NUMERICAL SOLUTION OF THE MULTIPOLE WAVE EQUATION

The wave equation (Equation (4-3) of the main text) is numerically solved by converting it to a secular equation as described in Reference E-1, Appendix E. We elaborate here only new details associated with the SO interaction.

To ensure that the numerically computed spin-orbit form factor (Equation (2-11) of the main text) has the correct transformation properties, we invoke the analogy

$$\vec{\nabla}' V(\vec{r}') \Leftrightarrow \vec{f}(\vec{r}') \quad (\text{E-1})$$

which follows from comparing with Equation (2-8) of the main text. In Equation (E-1),  $V(\vec{r}')$  transforms as a scalar under the groups  $D_{3d}$  or  $C_{3v}$ . Therefore, from Equation (2-8)

$$\vec{f}(\vec{G}') \Leftrightarrow i \vec{G}' V(\vec{G}') \quad (\text{E-2})$$

or

$$\vec{f}_{av}(\vec{G}') = i \vec{G}' \left[ \frac{\vec{G}' \cdot \vec{f}_c(\vec{G}')}{[\vec{G}' \cdot \vec{G}']} \right]_{av} \quad (\text{E-3})$$

In Equation (E-3),  $\vec{f}_c(\vec{G}')$  denotes the calculated spin-orbit form factor

and  $\left[ \frac{\vec{G}' \cdot \vec{f}_c(\vec{G}')}{[\vec{G}' \cdot \vec{G}']} \right]_{av}$  Equation (D-1) and is the average over all  $\vec{G}'$  vectors

---

E-1 Agassi, D. and Restorff, J. B., Pseudopotential Band Calculations Along a High-Symmetry Axis: Part I--Central Potential and the [111] Direction, NAVSWC TR 91-324, 15 Jun 1991 (unpublished).

which have the same  $|\vec{G}'_T|$ ,  $|\vec{G}'_Z|$ . If  $\vec{f}_c(\vec{G}')$  has the exact transformation properties, then  $\vec{f}_{av}(\vec{G}') = \vec{f}_c(\vec{G}')$ . Otherwise,  $\vec{f}_{av}(\vec{G}')$  has the correct transformation properties. The symmetrization Equation (E-3) has been used in all calculation.

The  $\sigma$ -mixing terms in Equation (4-3) are either proportional to  $f_m^{(z')}(g_p, z')$  or to the derivative  $\partial/\partial z'$ . Formally, the derivative appears in a hermitian combination (in  $\sigma$ ):  $f_m^{(+)}(z') \partial/\partial z'$  vs  $-f_m^{(-)}(z') \partial/\partial z'$  for  $\sigma=+1$  and  $\sigma=-1$  equations, respectively (the third term in Equation (4-3)). This hermiticity, however, is broken in the process of converting Equation (4-3) into a secular equation: As a consequence of our usage of sparse Fourier components, (which depend on  $g_0$  and  $g_F$ ), the set of bra-plane waves  $|m\rangle$  may be different from the ket-plane waves  $\langle m|$  (see Appendix E, Reference E-1) whereas the derivative acts always to the right. To correct for this artifact, we symmetrize the derivative term as follows ( $Q(z)$  is an arbitrary function):

$$\begin{aligned} \langle m| Q(z) \frac{\partial}{\partial z} |n\rangle &= \frac{1}{2} \langle m| \left[ \frac{\partial}{\partial z} \right] Q(z) + Q(z) \left[ \frac{\partial}{\partial z} \right] |n\rangle \\ &= \langle m| \left[ Q(z) \frac{\partial}{\partial z} \right]_S |n\rangle \end{aligned} \quad (E-3)$$

The substitution Equation (E-3) has its origin in the spin-orbit form, Equation (2-8). There the gradient operator acts to the right. Equivalently, the gradient can be made act to the left by commutation with the spin-orbit form factor, i.e.,

$$\vec{\nabla} v(\vec{r}) \times (\vec{\nabla})_L = -(\vec{\nabla})_R \times \vec{\nabla} v(\vec{r}) \quad (E-4)$$

where the left (L) and right (R) labels explicitly indicate the direction of the gradient operator. All subsequent calculations employ the symmetrized derivative form Equation (E-3).



DISTRIBUTION

	<u>Copies</u>		<u>Copies</u>
Office of the Chief of		Internal Distribution:	
Naval Research		E231	2
Attn: ONR-1114		E232	3
(Dr. G. Wright)	1	R41	1
(Dr. D. Liebenberg)	1	R41 (D. Agassi)	3
800 No. Quincy Street		R43 (J. Restorff)	1
Arlington, VA 22217-5000		R41 (T. Chu)	1
		R43 (K. Hathaway)	1
National Technical Information		R43 (J. Cullen)	1
Service (NTIS)			
Springfield, VA 22161	1		
Experimental Station			
DuPont de Nemours & Company			
Attn: R. V. Kasovski	1		
Wilmington, DE 19898			
Library of Congress			
Attn: Gift & Exchange Division	4		
Washington, DC 20540			
Defense Technical Information			
Center			
Cameron Station			
Alexandria, VA 22304-6145	12		

**REPORT DOCUMENTATION PAGE**Form Approved  
OMB No. 0704-0188

Public reporting burden for this collection of information is estimated to average 1 hour per response, including the time for reviewing instructions, searching existing data sources, gathering and maintaining the data needed, and completing and reviewing the collection of information. Send comments regarding this burden estimate or any other aspect of this collection of information, including suggestions for reducing this burden, to Washington Headquarters Services, Directorate for Information Operations and Reports, 1215 Jefferson Davis Highway, Suite 1204, Arlington, VA 22202-4302, and to the Office of Management and Budget, Paperwork Reduction Project (0704-0188), Washington, DC 20503

<b>1. AGENCY USE ONLY (Leave blank)</b>		<b>2. REPORT DATE</b> 1 July 1991	<b>3. REPORT TYPE AND DATES COVERED</b>	
<b>4. TITLE AND SUBTITLE</b> PSEUDOPOTENTIAL BAND CALCULATIONS ALONG A HIGH-SYMMETRY AXIS: PART II--Spin-Orbit Interaction and the [111] Direction			<b>5. FUNDING NUMBERS</b>	
<b>6. AUTHOR(S)</b> D. Y. Agassi and J. B. Restorff				
<b>7. PERFORMING ORGANIZATION NAME(S) AND ADDRESS(ES)</b> Naval Surface Warfare Center White Oak laboratory (Code R41) 10901 New Hampshire Avenue Silver Spring, MD 20903-5000			<b>8. PERFORMING ORGANIZATION REPORT NUMBER</b>  NAVSWC TR 91-326	
<b>9. SPONSORING/MONITORING AGENCY NAME(S) AND ADDRESS(ES)</b>			<b>10. SPONSORING/MONITORING AGENCY REPORT NUMBER</b>	
<b>11. SUPPLEMENTARY NOTES</b>				
<b>12a. DISTRIBUTION/AVAILABILITY STATEMENT</b>  Approved for public release; distribution is unlimited.			<b>12b. DISTRIBUTION CODE</b>	
<b>13. ABSTRACT (Maximum 200 words)</b>  A rapidly convergent method for band structure calculations, based on a cylindrical coordinates expansion, is generalized to include the spin-orbit interaction. This approach is advantageous particularly for materials highly anisotropic in one direction. The pertinent wave equations are tested for the PbSe low bands along the $\Gamma$ -L line. The results compare well with PbSe know band structure except where the bands group together to form degenerate, or near degenerate, equal parity clusters.				
<b>14. SUBJECT TERMS</b> high-symmetry axis      multipole expansion      wave equations superlattices          spin orbit interaction			<b>15. NUMBER OF PAGES</b> 53	
			<b>16. PRICE CODE</b>	
<b>17. SECURITY CLASSIFICATION OF REPORT</b> UNCLASSIFIED	<b>18. SECURITY CLASSIFICATION OF THIS PAGE</b> UNCLASSIFIED	<b>19. SECURITY CLASSIFICATION OF ABSTRACT</b> UNCLASSIFIED	<b>20. LIMITATION OF ABSTRACT</b> UL	

## GENERAL INSTRUCTIONS FOR COMPLETING SF 298

The Report Documentation Page (RDP) is used in announcing and cataloging reports. It is important that this information be consistent with the rest of the report, particularly the cover and its title page. Instructions for filling in each block of the form follow. It is important to *stay within the lines* to meet optical scanning requirements.

### Block 1. Agency Use Only (Leave blank).

**Block 2. Report Date.** Full publication date including day, month, and year, if available (e.g. 1 Jan 88). Must cite at least the year.

**Block 3. Type of Report and Dates Covered.** State whether report is interim, final, etc. If applicable, enter inclusive report dates (e.g. 10 Jun 87 - 30 Jun 88).

**Block 4. Title and Subtitle.** A title is taken from the part of the report that provides the most meaningful and complete information. When a report is prepared in more than one volume, repeat the primary title, add volume number, and include subtitle for the specific volume. On classified documents enter the title classification in parentheses.

**Block 5. Funding Numbers.** To include contract and grant numbers; may include program element number(s), project number(s), task number(s), and work unit number(s). Use the following labels:

C - Contract	PR - Project
G - Grant	TA - Task
PE - Program Element	WU - Work Unit Accession No.

**BLOCK 6. Author(s).** Name(s) of person(s) responsible for writing the report, performing the research, or credited with the content of the report. If editor or compiler, this should follow the name(s).

**Block 7. Performing Organization Name(s) and Address(es).** Self-explanatory.

**Block 8. Performing Organization Report Number.** Enter the unique alphanumeric report number(s) assigned by the organization performing the report.

**Block 9. Sponsoring/Monitoring Agency Name(s) and Address(es).** Self-explanatory.

**Block 10. Sponsoring/Monitoring Agency Report Number. (If Known)**

**Block 11. Supplementary Notes.** Enter information not included elsewhere such as: Prepared in cooperation with...; Trans. of...; To be published in... . When a report is revised, include a statement whether the new report supersedes or supplements the older report.

### Block 12a. Distribution/Availability Statement.

Denotes public availability or limitations. Cite any availability to the public. Enter additional limitations or special markings in all capitals (e.g. NOFORN, REL, ITAR).

**DOD** - See DoDD 5230.24, "Distribution Statements on Technical Documents."  
**DOE** - See authorities.  
**NASA** - See Handbook NHB 2200.2  
**NTIS** - Leave blank.

### Block 12b. Distribution Code.

**DOD** - Leave blank.  
**DOE** - Enter DOE distribution categories from the Standard Distribution for Unclassified Scientific and Technical Reports.  
**NASA** - Leave blank.  
**NTIS** - Leave blank.

**Block 13. Abstract.** Include a brief (**Maximum 200 words**) factual summary of the most significant information contained in the report.

**Block 14. Subject Terms.** Keywords or phrases identifying major subjects in the report.

**Block 15. Number of Pages.** Enter the total number of pages.

**Block 16. Price Code.** Enter appropriate price code (**NTIS only**)

**Blocks 17.-19. Security Classifications.** Self-explanatory. Enter U.S. Security Classification in accordance with U.S. Security Regulations (i.e., UNCLASSIFIED). If form contains classified information, stamp classification on the top and bottom of the page.

**Block 20. Limitation of Abstract.** This block must be completed to assign a limitation to the abstract. Enter either UL (unlimited) or SAR (same as report). An entry in this block is necessary if the abstract is to be limited. If blank, the abstract is assumed to be unlimited.